actions, recent studies have revealed that synovial cells have anabolic effects on the joint homeostasis, and differentiate into osteoblasts or chondrocytes under proper conditions.

In this review, I would like to introduce the role of osteoclasts in the joint destruction in RA, and the critical involvement of SFCs on the osteoclast differentiation in RA. Adenovirus vectors can efficiently transduce osteoclasts and SFCs both in vitro and in vivo. By modulating intracellular signaling pathways in these types of cells using adenovirus vectors, we could regulate the joint destruction in the experimental animal models of arthritis. We also successfully induced chondrogenic differentiation of SFCs both in vitro and in vivo by stimulating transforming growth factor (TGF)-β/bone morphogenetic protein (BMP) signaling pathways.

Involvement of osteoclasts in bone destruction in RA

The cellular mechanism underlying the bone and cartilage destruction in RA is still unclear, but emerging evidence has revealed the essential role of osteoclasts. Bromley and Woolley[6] observed a number of acid phosphatase-positive multinucleated cells (chondroclasts and/or osteoclasts) in the erosive joint areas of RA patients. Gravallese et al.[7] found that multinucleated cells present on erosive bone surface and in the areas of the direct invasion of pannus into the subchondral bone. Abundant multinucleated giant cells were also observed at the bone-pannus interfaces of arthritic joints in collagen-induced arthritis rats.[8] Multinucleated cells were positive for unique markers of osteoclasts such as tartrate-resistant acid phosphatase (TRAP), cathepsin K, and calcitonin receptors, satisfying the major criteria of mature osteoclasts.[7] Interestingly, some multinucleated cells and mononuclear cells apart from the bone surface were also TRAP-positive, suggesting the possible involvement of synovial tissues in the osteoclastogenesis in RA. To analyze the osteoclastogenic potentiality of RA synovial tissues, synovial cells were isolated from RA synovium at the time of knee replacement surgeries, and the cells were cultured in the presence of 1α,25-dihydroxyvitamin D_3 [$1,25(OH)_2D_3$] and macrophage colony-stimulating factor (M-CSF). After 3 weeks of culture, there appeared many multinucleated giant cells, which were TRAP-positive, possessed abundant calcitonin receptors, and made resorption pits on dentine slices.[9] We also found that peripheral monocytes can differentiate into osteoclast-like cells when cocultured with SFCs. These results suggest that RA SFCs can support osteoclast differentiation from monocyte-macrophage lineage precursor cells.

Role of RANKL/RANK pathways in bone destruction in RA

Receptor activator of NF-κB ligand (RANKL) is a member of the TNF superfamily cytokines, which was originally identified as a membrane-bound survival factor for dendritic cells produced by activated T cells.[10,11] The expression of RANKL is also induced in osteoblasts or bone marrow stromal cells by various hormones or cytokines. In cooperation with M-CSF, RANKL stimulates osteoclast differentiation from hematopoietic precursor cells in vitro.[12] RANKL also acts on mature osteoclasts and promotes their bone-resorbing activity and survival. RANKL binds to its specific receptor RANK, the type I membrane receptor belonging to TNF receptor superfamily. RANK is expressed in wide range of cells including monocyte-macrophage lineage osteoclast precursor cells, mature osteoclasts and dendritic cells. Upon binding to its ligand RANKL, RANK recruits an adaptor molecule TNF receptor-associated factor (TRAF) 6, which subsequently activates downstream signaling pathways NF-κB, c-Jun N-terminus kinase (JNK), p38 mitogen-activated protein (MAP) kinase, and nuclear factor of activated T cells (NFAT) c1.[13] Another important actor in the RANKL/RANK pathway is osteoprotegerin (OPG), a soluble decoy receptor of RANKL which belongs to TNF receptor superfamily.[14,15] Osteoprotegerin specifically binds to RANKL and inhibits RANKL activity by competitively preventing its binding to RANK.

The essential role of RANKL/RANK signaling pathways in osteoclast development was further established by a series of gene knockout mice.[16] The targeted disruption of either RANKL or RANK induced osteopetrosis in mice, a pathological bone disease which is characterized by an increased bone mass due to a deficiency in osteoclast differentiation.[11,16] We and another group found that mice deficient in TRAF6 also showed osteopetrotic phenotypes.[17] In contrast, OPG-deficient animals demonstrated osteopenia due to the increased number and activity of osteoclasts.[18,19] These results clearly demonstrate the essential role of RANKL/RANK pathways in osteoclast development and activation in vivo.

Not only is the RANKL/RANK pathway critical for normal bone development and growth, but also is implicated in the pathological bone resorption observed in RA (Fig. 1). We and other groups found a high level expression of RANKL in RA synovial tissues.[20,21] Enhanced expression of RANKL is observed in SFCs as well as in $CD4^+$ T lymphocytes in synovial tissues of collagen-induced arthritis rats as shown by in situ hybridization.[22] Expression of RANKL is increased by T-cell proinflammatory cytokine IL-17, and IL-17 enhanced RANKL expression and strongly upregulated the RANKL/OPG ratio in the synovium.[23] Osteoprotegerin treatment ameliorates the arthritic bone destruction in adjuvant arthritis rats[24] and TNF-α transgenic animals,[25] and the bone erosion in serum transfer-induced arthritis was markedly reduced in RANKL-deficient animals.[26] Recent studies also demonstrated that the systemic bone loss as well as the local bone erosion in TNF-α transgenic mice was reversed by OPG injection in combination with anti-TNF-α antibody therapy.[27,28] These studies indicate that RANKL produced by SFCs and/or activated T lymphocytes in RA synovial tissues plays an essential role in the osteoclast development and the joint destruction, and therefore, the RANKL/RANK pathway can be a good therapeutic target.

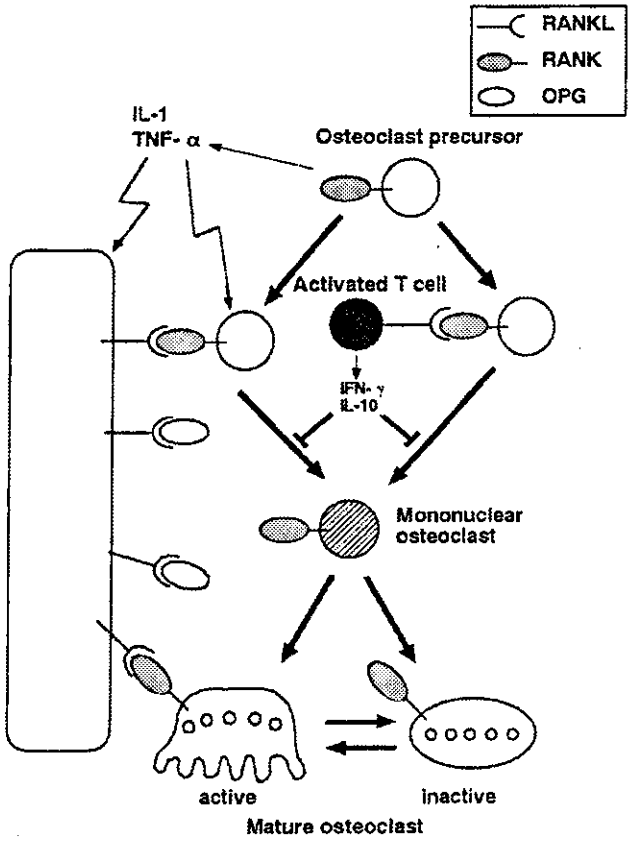

Fig. 1. Involvement of receptor activator of NF-κB ligand (*RANKL*)–receptor activator of NF-κB (*RANK*) pathways in osteoclast differentiation and bone destruction in RA. RANKL is highly expressed in synovial fibroblastic cells (SFCs) and activated T cells, and binds to its specific receptor RANK, which is expressed in monocyte-macrophage lineage osteoclast precursor cells. The interaction between RANKL and RANK is blocked by osteoprotegerin (*OPG*), a physiological inhibitor of RANKL. *IL*, interleukin; *TNF*, tumor necrosis factor; *IFN*, interferon

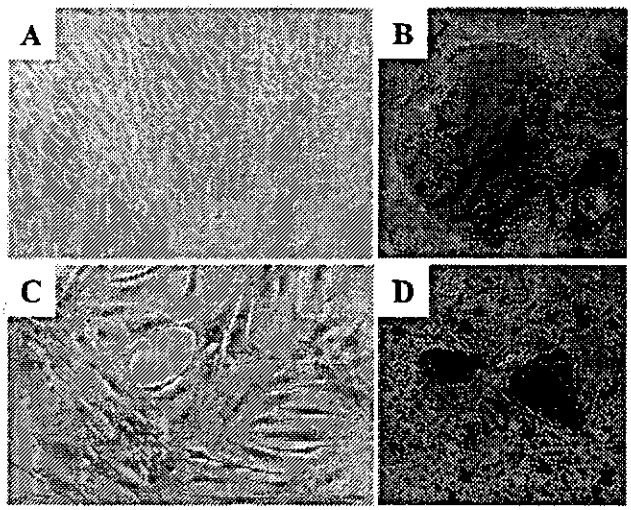

Fig. 2A–D. Effective gene transduction into SFCs and mature osteoclasts by adenovirus vectors. Human SFCs obtained from synovial tissues of rheumatoid arthritis patients (**A** and **C**) or osteoclast-like cells from giant cell tumors (**B** and **D**) were infected with the control virus (**A** and **B**) or LacZ virus (**C** and **D**), and stained for β-galactosidase activity 1 day after infection. Both SFCs and osteoclasts infected with LacZ virus were positively stained, indicating an efficient gene transduction

Efficiency of adenovirus vectors in transducing SFCs and osteoclasts

As mentioned above, osteoclasts play pivotal roles in the bone and joint pathology in RA, and SFCs support osteoclast differentiation and activation by producing RANKL. Therefore, pharmacological agents targeting these cells can be potent therapeutic candidates for the treatment of RA. One alternative is gene therapy, where genes or cDNAs are directly transferred to target cells. In preclinical studies, ex vivo and in vivo gene transfer methods have been used successfully to reduce the joint destruction in experimental arthritis, and the first clinical trial, in which the IL-1 receptor antagonist gene was delivered to synoviocytes ex vivo, was started in 1996 in the United States.[29,30] The proper selection of the target cells and target genes has been a continuous matter of interest for successful gene therapies. The target cells for the RA gene therapy include SFCs and osteoclasts, and we previously reported that adenovirus vectors efficiently transduce foreign genes into these cells both in vitro and in vivo.[31,32] As shown in Fig. 2, recombinant adenovirus vectors carrying the *lacZ* gene can infect human SFCs and osteoclast-like cells obtained from giant cell tumors.[31,32] At a multiplicity of infection of 100, almost 100% of SFCs and more than 85% of osteoclast-like cells were positively stained by β-galactosidase (β-gal) activity with no apparent morphological changes or cellular toxicity. When injected into knee joints of adjuvant arthritis rats, synovial lining cells and osteoclasts present on bone surface were positively stained for β-gal activity (Fig. 3).[32] These results suggest that the adenovirus vector system is suitable for gene therapies targeting SFCs and osteoclasts. As for target molecules, we focused on the intracellular signaling pathways which are important for both SFCs and osteoclasts, i.e., c-Src pathways and Ras/ERK pathways.

Adenovirus vector-mediated regulation of c-Src pathways in SFCs and osteoclasts

c-Src was first identified as the normal cellular counterpart of the transforming protein encoded by Rous sarcoma virus, v-Src.[33] The protooncogene product c-Src is a 60 kDa protein and belongs to non-receptor-type tyrosine kinase family, i.e., Src family tyrosine kinase family. The *c-src* protooncogene is highly conserved throughout evolution and widely expressed. It is known that c-Src and the other members of the Src family, which share highly conserved sequences both within and outside the kinase catalytic domain, play important roles in signal transduction mecha-

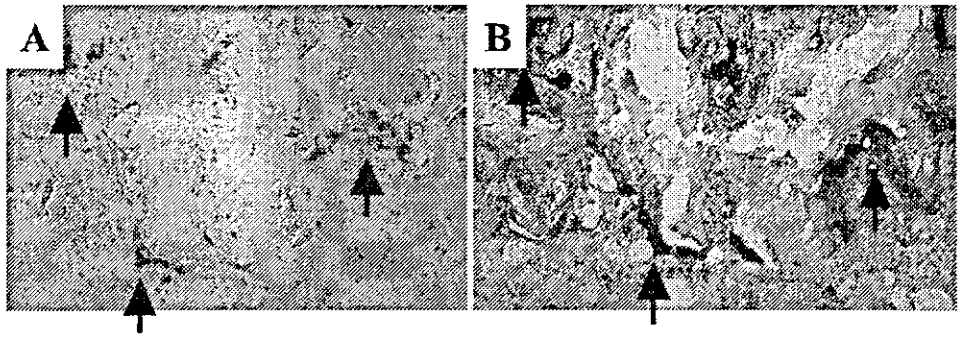

Fig. 3A,B. Adenovirus-mediated gene transduction in osteoclasts in vivo.[43] LacZ virus was injected into the inflammatory ankle joint of an adjuvant arthritis rat, and the expression *lacZ* gene in osteoclasts was determined in the serial sections by enzyme histochemistry of β-galactosidase (**A**) and tartrate-resistant acid phosphatase (TRAP) (**B**) after 1 week of the viral injection. Most of the TRAP-positive osteoclasts were positively stained for β-galactosidase activity

nisms that contribute to the regulation of cell growth and development.[33] The physiological role of the c-*src* gene had not been clarified until Soriano et al. successfully performed the targeted disruption of the gene by homologous recombination in mouse embryos in 1991.[34] To everyone's surprise, the mice showed striking skeletal abnormalities with a phenotype of osteopetrosis. In vitro osteoclast formation experiments and in vivo bone marrow transplantation studies have revealed that osteoclast differentiation was not impaired, but that bone-resorbing activity of mature osteoclasts was much reduced in c-*src* knockout (KO) mice.[35,36] The morphological feature of the KO osteoclasts was their disorganized ruffled border structure.[36] The ruffled border is the apical membrane of the osteoclast, which is extensively folded due to the intense vesicular traffic associated with proton and lysosomal enzyme secretion. c-Src is highly expressed in osteoclasts, and highly concentrated on ruffled border membranes and intracellular membranes.[37,38] The fact that no other abnormalities in c-*src* KO mice were found outside the skeletal tissues leads us to consider that c-Src can be an ideal therapeutic target for suppressing pathological bone resorption by inhibiting osteoclast function without affecting other tissues or cells.

The tyrosine kinase activity of c-Src is strictly regulated by phosphorylation and dephosphorylation of the tyrosine residue located close to the C-terminus, which corresponds to tyrosine 527 (Tyr527) in chicken c-Src.[39] Dephosphorylation of this residue causes a 10- to 20-fold increase in the kinase activity of c-Src. C-terminus Src family kinase (Csk) is a cytoplasmic tyrosine kinase which specifically phosphorylates Tyr527 of c-Src, thereby negatively regulate its kinase activity.[40] To regulate c-Src kinase activity in SFCs and osteoclasts, we constructed adenovirus vectors encoding *csk* gene (Csk virus). Csk virus efficiently infected SFCs and osteoclasts, and dose-dependently inhibited the kinase activity of c-Src in these cells.[41] Adenovirus vector-mediated Csk overexpression in RA SFCs suppressed the proliferation of the cells, and reduced their IL-6 production.[32] Csk virus also induced dramatic cytoskeletal disorganization in osteoclasts, and strongly inhibited pit formation on dentine slices.[41]

Important role of Ras/ERK pathways in SFC activation and osteoclast survival

The other signaling pathway we focused on as a therapeutic target is the Ras/ERK pathway. Small GTPase Ras, the protein product of proto-oncogene *ras*, is ubiquitously found in eukaryotic organisms.[42] Ras is known to function as a downstream effector of cell surface receptor tyrosine kinases (RTKs) and leads to the activation of ERK pathways, which in turn regulates the activities of nuclear transcription factors and gene transcriptions. In human cancer cells, oncogenic mutations of Ras protein are frequently observed and contribute to the malignant growth properties of the cells. In RA and animal models of arthritis, synovial cells with large pale nuclei, prominent nucleoli and abundant cytoplasm are found adjacent to the affected cartilage and bone of the joint, and these cells in culture have a tendency to grow in disorganized monolayers, proliferate in an anchorage-independent manner, lack contact inhibition, and form microfoci, exhibiting a morphologically transformed appearance.[4] Although the expression of Ras and its oncogenic mutations were reported in RA synovial cells, the precise role of Ras in RA pathology remains unclear.[43] To analyze the role of Ras and its downstream signaling in osteoclasts as well as in SFCs, we constructed a replication-deficient adenovirus vector carrying the dominant negative mutant of *ras* gene (Ras^{DN}). In SFCs, adenovirus-mediated overexpression of Ras^{DN} dramatically decreased the proliferation rate of the cells. Interleukin-1-induced upregulation of IL-6 production was also decreased by the viral infection, which was supposedly mediated by the downregulation of IL-1-induced ERK activation.[44]

In addition, the life span of osteoclasts was markedly decreased by the adenovirus, while activating Ras/ERK pathways by constitutively active mutant of ERK expression prolonged the survival of osteoclasts.[45] These results suggest that Ras/ERK pathways are critically involved in SFC activation and osteoclast survival.

Amelioration of arthritic bone destruction by adenovirus vector-induced gene expression

The efficient in vivo gene delivery to synovial cells by local administration of adenovirus vectors has been well established.[32,46] In addition, TRAP-positive osteoclasts along the erosive bone surface demonstrated strong β-gal staining as shown in the serial tissue sections, indicating that intra-articular injection of adenovirus vectors can transduce osteoclasts in vivo (Fig. 3). The effect of Csk and Ras^{DN} adenovirus administration into inflammatory ankle joints of adjuvant arthritis rats was investigated.[32,44] Not only was the bone destruction by osteoclasts suppressed by Csk or Ras^{DN} virus injection, but also the synovial inflammatory reaction detected by arthritis score or paw swelling was reduced (Fig. 4). These results lead us to conclude that regulating c-Src and/or Ras/ERK pathways in SFCs and osteoclasts can be a novel therapeutic approach to treat RA joint destruction (Fig. 5).

Stimulating chondrogenic differentiation of SFCs

In contrast to such catabolic actions, recent studies have revealed that SFCs have anabolic effects, leading to the bone and cartilage production. Hunziker and Rosenberg[47] reported that synovial cells can migrate into partial-thickness articular cartilage defects, where they proliferate and subsequently deposit a scar-like tissue. Nishimura et al.[48] demonstrated SFCs to show chondrogenic differentiation after being cultured in the presence of TGF-β, and De Bari et al.[49] recently demonstrated that multipotent mesenchymal stem cells were isolated from human synovial tissues, which differentiated into chondrocytes as well as osteoblasts, adipocytes, and myotubes under proper culture conditions. These observations lead us to speculate that synovial tissues contain multipotent cells with osteogenic and/or chondrogenic potential that can be involved in the repair process of destroyed joints and therefore might provide a good source for engineering the bone and cartilage.

There is accumulating evidence that TGF-β superfamily cytokines play an essential role in bone and cartilage development. We analyzed the role of TGF-β/BMP signaling on chondrogenic differentiation of human SFCs, and found that the introduction of an activated mutant of ALK3 (con-

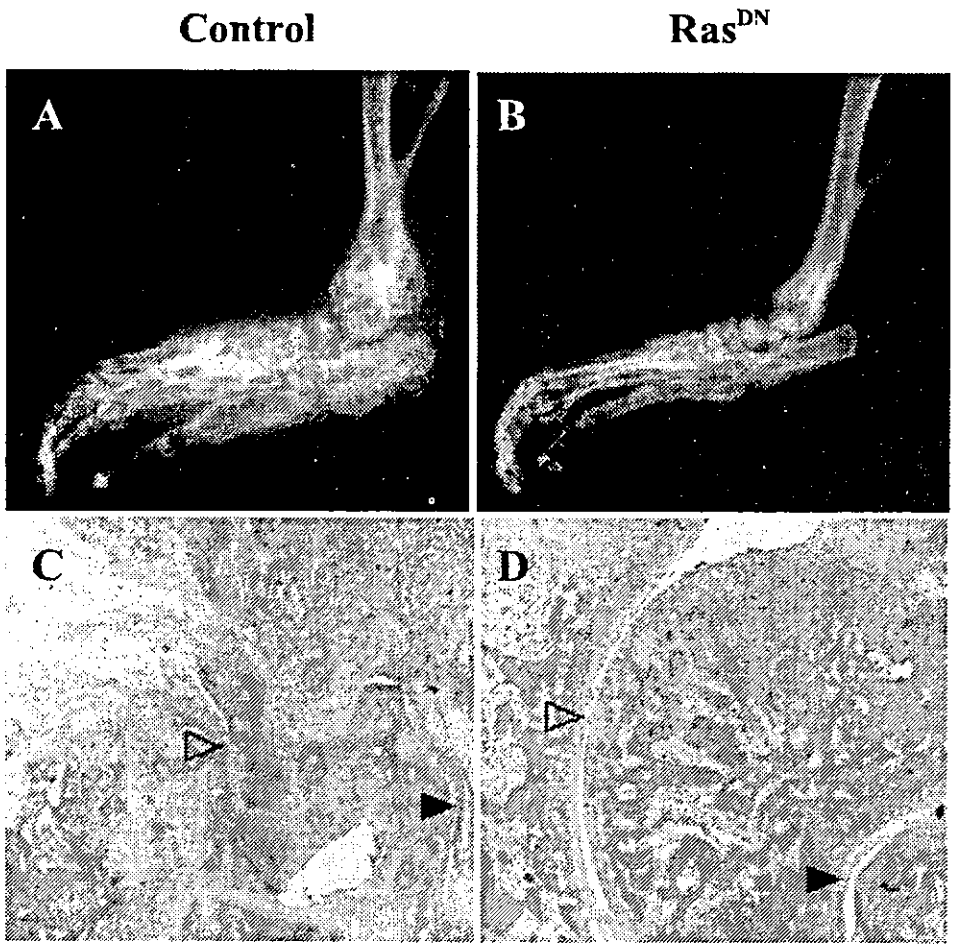

Fig. 4A–D. Therapeutic effects of dominant negative Ras (*Ras^{DN}*) adenovirus injection on rat adjuvant arthritis. **A,B** The radiological findings of the ankle of LacZ virus- (**A**) and Ras^{DN} virus- (**B**) injected rats. Severe joint destruction could be seen in LacZ virus-injected rats, while Ras^{DN} virus-injected ankle joints show minimal destructive changes. **C** Pathohistological findings of the LacZ virus-injected ankles show synovial hyperplasia and destructive change of articular cartilage and bone. *Open arrowhead* and *closed arrowhead* indicate talo-tibial and talo-calcaneal joint, respectively. **D** Pathohistological findings of the Ras^{DN} virus-injected ankle. Synovial hyperplasia with invasion into subchondral bone and the destruction of bone and cartilage were markedly suppressed. **C,D**: H&E staining

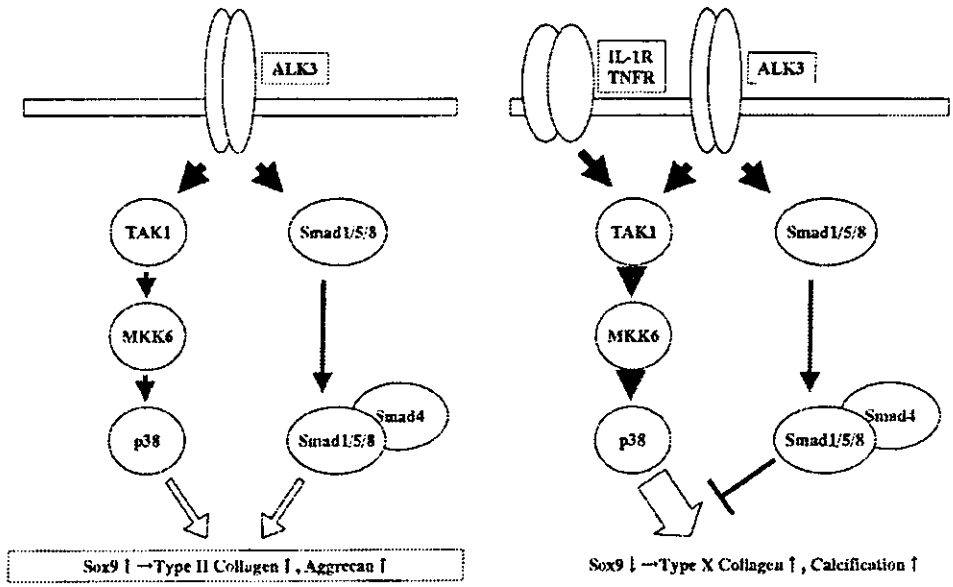

Fig. 7. The role of the Smad pathway and p38 mitogen-activated protein kinase pathway on chondrogenic differentiation of SFCs. Although both pathways are necessary for chondrocyte-specific marker expression in the cells (*left panel*), overactivation of p38 pathways alone lead to the terminal chondrocytic differentiation of the cells, leading to the articular cartilage degeneration. The proper balance between these two pathways is required for maintaining the articular cartilage integrity. *IL*, interleukin; *TNFR*, tumor necrosis factor receptor; *ALK*, activin receptor-like kinase

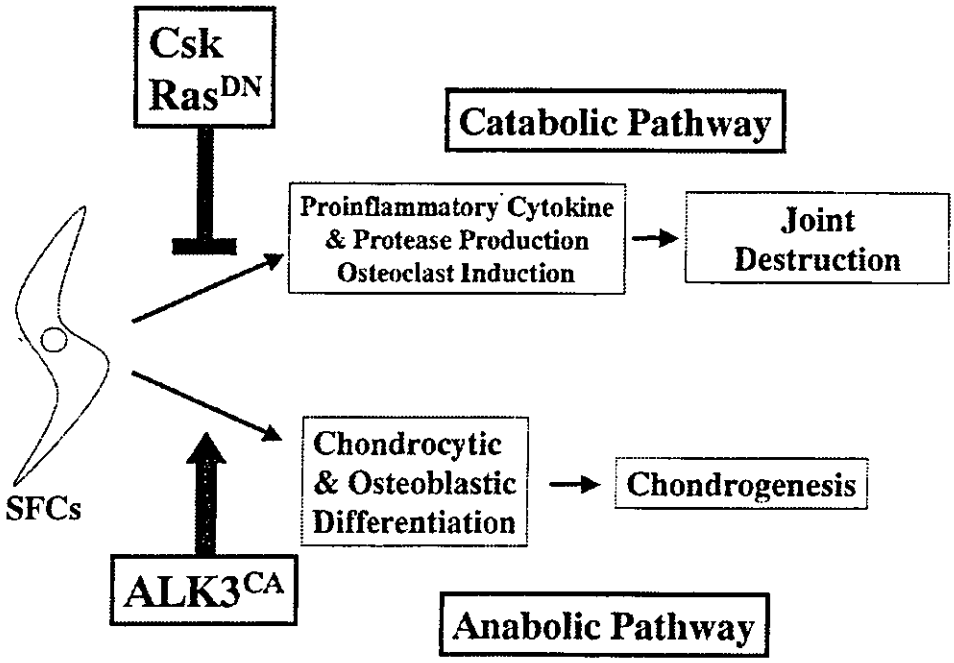

Fig. 8. Schematic representation of the therapeutic strategies targeting synovial fibroblastic cells (*SFCs*). Suppressing Src pathways by C-terminal Src family kinase (*Csk*) expression or Ras/ERK pathways by dominant negative Ras (Ras^{DN}) expression suppresses the catabolic pathways of the cells which lead to the bone and joint destruction in RA, while stimulating ALK3 pathways activates anabolic pathways leading to chondrogenic differentiation of the cells. $ALK3^{CA}$, constitutively active activin receptor-like kinase

differentiation of SFs, but also regulate the stage of differentiation of the cells and suppress their terminal differentiation process. It should be noted that the proinflammatory cytokines IL-1 and TNF-α, which are known to have catabolic effects on joint integrity, induced p38 activation in SFs.[52] These cytokines may stimulate terminal chondrogenic differentiation of SFs which are involved in the repair process, and lead to the articular cartilage degradation. Based on our observation, we would like to propose that SFs are an excellent source from which to obtain chondroprogenitors, which can be differentiated into chondrocytes via ALK3 activation, and that stimulating Smad pathways and controlling p38 activation to the proper level can be a good therapeutic strategy for maintaining the healthy joint homeostasis and treating degenerative joint disorders.

Concluding remarks

The ultimate goal of the treatment of RA is to preserve the daily activity of the patients by preventing bone and joint destruction. Recent studies have revealed that osteoclasts are involved in the pathogenesis of the bone and joint destruction in RA, and SFCs are critically involved in the differentiation and activation of osteoclasts by producing various catabolic factors including TNF-α, IL-1, and RANKL, which makes osteoclasts and SFCs good therapeutic targets for bone and joint destruction in RA. We demonstrated that suppressing Src pathways by introducing Csk and/or Ras/ERK pathways by the Ras^{DN} adenovirus in osteoclasts reduces bone resorption both in vitro or in vivo by suppressing osteoclast activity or survival (Fig. 5). Csk virus and Ras^{DN} virus also suppress catabolic actions of SFCs by inhibiting abnormal proliferation of the cells and their IL-6 production (Fig. 5). We also succeeded to stimulate chondrogenic differentiation of SFCs by introducing $ALK3^{CA}$, and the proper balance of the Smad pathway and the p38 MAP kinase pathway is critical downstream of ALK3. Based on these observations, I would like to propose that modulating intracellular signaling in osteoclasts and/or SFCs by adenovirus vectors can be good therapeutic approach for treating RA patients with bone and joint destruction (Fig. 8).

Of course, we have to realize the disadvantages as well as advantages of using adenovirus vectors as therapeutic reagents.[53] The disadvantages of the adenovirus vectors include the transient gene expression because they do not integrate the transgene into target cell chromosome, immunological reaction such as neutralizing antibody response and cytotoxic T-lymphocyte responses against the virus, and the dissemination of the vectors from the site of local injection.[54] The safety issue is particularly important regarding its clinical application, and in fact, the first case of fatality induced by the infusion of adenovirus vectors into hepatic artery was recently reported. Therefore, development of a new generation of adenovirus vectors or finding substitutes for gene therapy is absolutely necessary for the clinical application of the signaling molecule-targeting strategies.

Acknowledgments This work was in part supported by Grants-in-Aid from the Ministry of Education, Culture, Sports, Science, and Technology of Japan, and Health Science Research Grants from the Ministry of Health, Labour and Welfare, to S.T.

References

1. Firestein GS. Evolving concepts of rheumatoid arthritis. Nature 2003;423:356–61.
2. Lipsky PE, van der Heijde DM, St Clair EW, Furst DE, Breedveld FC, Kalden JR, et al. Infliximab and methotrexate in the treatment of rheumatoid arthritis. Anti-Tumor Necrosis Factor Trial in Rheumatoid Arthritis with Concomitant Therapy Study Group. N Engl J Med 2000;343:1594–602.
3. Sorsa T, Konttinen YT, Lindy O, Ritchlin C, Saari H, Suomalainen K, et al. Collagenase in synovitis of rheumatoid arthritis. Semin Arthritis Rheum 1992;22:44–53.
4. Firestein GS. Invasive fibroblast-like synoviocytes in rheumatoid arthritis. Passive responders or transformed aggressors? Arthritis Rheum 1996;39:1781–90.
5. Muller-Ladner U, Kriegsmann J, Gay RE, Gay S. Oncogenes in rheumatoid arthritis. Rheum Dis Clin North Am 1995;21:675–90.
6. Bromley M, Woolley DE. Chondroclasts and osteoclasts at subchondral sites of erosion in the rheumatoid joint. Arthritis Rheum 1984;27:968–75.
7. Gravallese EM, Harada Y, Wang JT, Gorn AH, Thornhill TS, Goldring SR. Identification of cell types responsible for bone resorption in rheumatoid arthritis and juvenile rheumatoid arthritis. Am J Pathol 1998;152:943–51.
8. Suzuki Y, Nishikaku F, Nakatuka M, Koga Y. Osteoclast-like cells in murine collagen induced arthritis. J Rheumatol 1998;25:1154–60.
9. Takayanagi H, Oda H, Yamamoto S, Kawaguchi H, Tanaka S, Nishikawa T, et al. A new mechanism of bone destruction in rheumatoid arthritis: synovial fibroblasts induce osteoclastogenesis. Biochem Biophys Res Commun 1997;240:279–86.
10. Wong BR, Josien R, Choi Y. TRANCE is a TNF family member that regulates dendritic cell and osteoclast function. J Leukocyte Biol 1999;65:715–24.
11. Suda T, Takahashi N, Udagawa N, Jimi E, Gillespie MT, Martin TJ. Modulation of osteoclast differentiation and function by the new members of the tumor necrosis factor receptor and ligand families. Endocr Rev 1999;20:345–57.
12. Yasuda H, Shima N, Nakagawa N, Yamaguchi K, Kinosaki M, Mochizuki S, et al. Osteoclast differentiation factor is a ligand for osteoprotegerin/osteoclastogenesis-inhibitory factor and is identical to TRANCE/RANKL. Proc Natl Acad Sci USA 1998;95:3597–602.
13. Tanaka S, Nakamura I, Inoue J, Oda H, Nakamura K. Signal transduction pathways regulating osteoclast differentiation and function. J Bone Miner Metab 2003;21:123–33.
14. Tsuda E, Goto M, Mochizuki S, Yano K, Kobayashi F, Morinaga T, et al. Isolation of a novel cytokine from human fibroblasts that specifically inhibits osteoclastogenesis. Biochem Biophys Res Commun 1997;234:137–42.
15. Simonet WS, Lacey DL, Dunstan CR, Kelley M, Chang MS, Luthy R, et al. Osteoprotegerin: a novel secreted protein involved in the regulation of bone density. Cell 1997;89:309–19.
16. Boyle WJ, Simonet WS, Lacey DL. Osteoclast differentiation and activation. Nature 2003;423:337–42.
17. Inoue J, Ishida T, Tsukamoto N, Kobayashi N, Naito A, Azuma S, et al. Tumor necrosis factor receptor-associated factor (TRAF) family: adapter proteins that mediate cytokine signaling. Exp Cell Res 2000;254:14–24.
18. Bucay N, Sarosi I, Dunstan CR, Morony S, Tarpley J, Capparelli C, et al. osteoprotegerin-deficient mice develop early onset osteoporosis and arterial calcification. Genes Dev 1998;12:1260–8.
19. Mizuno A, Amizuka N, Irie K, Murakami A, Fujise N, Kanno T, et al. Severe osteoporosis in mice lacking osteoclastogenesis inhibitory factor/osteoprotegerin. Biochem Biophys Res Commun 1998;247:610–5.
20. Takayanagi H, Iizuka H, Juji T, Nakagawa T, Yamamoto A, Miyazaki T, et al. Involvement of receptor activator of nuclear factor kappaB ligand/osteoclast differentiation factor in osteoclastogenesis from synoviocytes in rheumatoid arthritis. Arthritis Rheum 2000;43:259–69.
21. Gravallese EM, Manning C, Tsay A, Naito A, Pan C, Amento E, et al. Synovial tissue in rheumatoid arthritis is a source of osteoclast differentiation factor. Arthritis Rheum 2000;43:250–8.
22. Romas E, Bakharevski O, Hards DK, Kartsogiannis V, Quinn JM, Ryan PF, et al. Expression of osteoclast differentiation factor at sites of bone erosion in collagen-induced arthritis. Arthritis Rheum 2000;43:821–6.
23. Lubberts E, van den Bersselaar L, Oppers-Walgreen B, Schwarzenberger P, Coenen-de Roo CJ, Kolls JK, et al. IL-17 promotes bone erosion in murine collagen-induced arthritis through loss of the receptor activator of NF-kappa B ligand/osteoprotegerin balance. J Immunol 2003;170:2655–62.
24. Kong YY, Feige U, Sarosi I, Bolon B, Tafuri A, Morony S, et al. Activated T cells regulate bone loss and joint destruction in adjuvant arthritis through osteoprotegerin ligand. Nature 1999;402:304–9.

25. Redlich K, Hayer S, Maier A, Dunstan CR, Tohidast-Akrad M, Lang S, et al. Tumor necrosis factor alpha-mediated joint destruction is inhibited by targeting osteoclasts with osteoprotegerin. Arthritis Rheum 2002;46:785–92.
26. Pettit AR, Ji H, von Stechow D, Muller R, Goldring SR, Choi Y, et al. TRANCE/RANKL knockout mice are protected from bone erosion in a serum transfer model of arthritis. Am J Pathol 2001;159:1689–99.
27. Redlich K, Gortz B, Hayer S, Zwerina J, Doerr N, Kostenuik P, et al. Repair of local bone erosions and reversal of systemic bone loss upon therapy with anti-tumor necrosis factor in combination with osteoprotegerin or parathyroid hormone in tumor necrosis factor-mediated arthritis. Am J Pathol 2004;164:543–55.
28. Zwerina J, Hayer S, Tohidast-Akrad M, Bergmeister H, Redlich K, Feige U, et al. Single and combined inhibition of tumor necrosis factor, interleukin-1, and RANKL pathways in tumor necrosis factor-induced arthritis: effects on synovial inflammation, bone erosion, and cartilage destruction. Arthritis Rheum 2004;50:277–90.
29. Evans CH, Ghivizzani SC, Herndon JH, Wasko MC, Reinecke J, Wehling P, et al. Clinical trials in the gene therapy of arthritis. Clin Orthop 2000:S300–7.
30. Evans CH, Gouze JN, Gouze E, Robbins PD, Ghivizzani SC. Osteoarthritis gene therapy. Gene Ther 2004;11:379–89.
31. Tanaka S, Takahashi T, Takayanagi H, Miyazaki T, Oda H, Nakamura K, et al. Modulation of osteoclast function by adenovirus vector-induced epidermal growth factor receptor. J Bone Miner Res 1998;13:1714–20.
32. Takayanagi H, Juji T, Miyazaki T, Iizuka H, Takahashi T, Isshiki M, et al. Suppression of arthritic bone destruction by adenovirus-mediated csk gene transfer to synoviocytes and osteoclasts. J Clin Invest 1999;104:137–46.
33. Thomas SM, Brugge JS. Cellular functions regulated by Src family kinases. Annu Rev Cell Dev Biol 1997;13:513–609.
34. Soriano P, Montgomery C, Geske R, Bradley A. Targeted disruption of the c-src proto-oncogene leads to osteopetrosis in mice. Cell 1991;64:693–702.
35. Lowe C, Yoneda T, Boyce BF, Chen H, Mundy GR, Soriano P. Osteopetrosis in Src-deficient mice is due to an autonomous defect of osteoclasts. Proc Natl Acad Sci USA 1993;90:4485–9.
36. Boyce BF, Yoneda T, Lowe C, Soriano P, Mundy GR. Requirement of pp60c-src expression for osteoclasts to form ruffled borders and resorb bone in mice. J Clin Invest 1992;90:1622–7.
37. Horne WC, Neff L, Chatterjee D, Lomri A, Levy JB, Baron R. Osteoclasts express high levels of pp60c-src in association with intracellular membranes. J Cell Biol 1992;119:1003–13.
38. Tanaka S, Takahashi N, Udagawa N, Sasaki T, Fukui Y, Kurokawa T, et al. Osteoclasts express high levels of p60c-src, preferentially on ruffled border membranes. FEBS Lett 1992;313:85–9.
39. Brown MT, Cooper JA. Regulation, substrates and functions of src. Biochim Biophys Acta 1996;1287:121–49.
40. Okada M, Nada S, Yamanashi Y, Yamamoto T, Nakagawa H. CSK: a protein-tyrosine kinase involved in regulation of src family kinases. J Biol Chem 1991;266:24249–52.
41. Miyazaki T, Takayanagi H, Isshiki M, Takahashi T, Okada M, Fukui Y, et al. In vitro and in vivo suppression of osteoclast function by adenovirus vector-induced csk gene. J Bone Miner Res 2000;15:41–51.
42. Bourne HR, Sanders DA, McCormick F. The GTPase superfamily: conserved structure and molecular mechanism. Nature 1991;349:117–27.
43. Gay S, Gay RE. Cellular basis and oncogene expression of rheumatoid joint destruction. Rheumatol Int 1989;9:105–13.
44. Yamamoto A, Fukuda A, Seto H, Miyazaki T, Kadono Y, Sawada Y, et al. Suppression of arthritic bone destruction by adenovirus-mediated dominant-negative Ras gene transfer to synoviocytes and osteoclasts. Arthritis Rheum 2003;48:2682–92.
45. Miyazaki T, Katagiri H, Kanegae Y, Takayanagi H, Sawada Y, Yamamoto A, et al. Reciprocal role of ERK and NF-kappaB pathways in survival and activation of osteoclasts. J Cell Biol 2000;148:333–42.
46. Nita I, Ghivizzani SC, Galea-Lauri J, Bandara G, Georgescu HI, Robbins PD, et al. Direct gene delivery to synovium. An evaluation of potential vectors in vitro and in vivo. Arthritis Rheum 1996;39:820–8.
47. Hunziker EB, Rosenberg LC. Repair of partial-thickness defects in articular cartilage: cell recruitment from the synovial membrane. J Bone Joint Surg Am 1996;78:721–33.
48. Nishimura K, Solchaga LA, Caplan AI, Yoo JU, Goldberg VM, Johnstone B. Chondroprogenitor cells of synovial tissue. Arthritis Rheum 1999;42:2631–7.
49. De Bari C, Dell'Accio F, Tylzanowski P, Luyten FP. Multipotent mesenchymal stem cells from adult human synovial membrane. Arthritis Rheum 2001;44:1928–42.
50. Seto H, Kamekura S, Miura T, Yamamoto A, Chikuda H, Ogata T, et al. Distinct roles of Smad pathways and p38 pathways in cartilage-specific gene expression in synovial fibroblasts. J Clin Invest 2004;113:718–26.
51. Zhen X, Wei L, Wu Q, Zhang Y, Chen Q. Mitogen-activated protein kinase p38 mediates regulation of chondrocyte differentiation by parathyroid hormone. J Biol Chem 2001;276:4879–85.
52. Schett G, Tohidast-Akrad M, Smolen JS, Schmid BJ, Steiner CW, Bitzan P, et al. Activation, differential localization, and regulation of the stress-activated protein kinases, extracellular signal-regulated kinase, c-JUN N-terminal kinase, and p38 mitogen-activated protein kinase, in synovial tissue and cells in rheumatoid arthritis. Arthritis Rheum 2000;43:2501–12.
53. Mountain A. Gene therapy: the first decade. Trends Biotechnol 2000;18:119–28.
54. Benihoud K, Yeh P, Perricaudet M. Adenovirus vectors for gene delivery. Curr Opin Biotechnol 1999;10:440–7.

Osteoporos Int (2005) 16: 64–70
DOI 10.1007/s00198-004-1642-1

ORIGINAL ARTICLE

Significance of intima-media thickness in femoral artery in the determination of calcaneus osteo-sono index but not of lumbar spine bone mass in healthy Japanese people

Shinsuke Yamada · Masaaki Inaba · Hitoshi Goto
Mayumi Nagata · Misako Ueda · Kiyoshi Nakatuka
Hideki Tahara · Hisayo Yokoyama · Masanori Emoto
Tetsuo Shoji · Yoshiki Nishizawa

Received: 16 April 2003 / Accepted: 19 March 2004 / Published online: 27 May 2004

Abstract The aim of this cross-sectional study was to investigate whether physical activity and local arterial thickening may affect bone metabolism. To analyze the effects of physical activity and atherosclerosis on bone in healthy Japanese people, health-related quality of life (HRQL) and local arterial thickening were assessed by means of the MedicalOutcomes Study 36-item Short Form (SF-36), and intimal-medial thickness (IMT) in common carotid artery (CA) and femoral artery (FA), respectively. Bone mineral density (BMD) in lumbar spine was measured by dual X-ray absorptiometry and the osteo-sono assessment index (OSI) of the calcaneus by ultrasound. Healthy subjects (106 male and 154 female) were recruited from those who participated in a local health check program at the Osaka City University Hospital. A significant correlation existed between lumbar spine BMD and calcaneus OSI ($r=0.551$, $P<0.0001$). Among various scores in SF-36, only physical functioning score correlated weakly but significantly in a positive manner with lumbar spine BMD ($\rho=0.156$, $P=0.0147$) and calcaneus OSI ($\rho=0.190$, $P=0.0024$). Lumbar spine BMD correlated negatively with FA IMT ($\rho=-0.191$, $P=0.0027$) whereas calcaneus OSI with FA IMT ($\rho=-0.199$, $P=0.0014$). Multiple regression analyses revealed a significant association between FA IMT and calcaneus OSI, whereas lumbar spine BMD did not correlate significantly with FA or CA IMT. When subjects were restricted to female, FA IMT, but not CA IMT, still showed tendency against independent factors negatively associated with calcaneus OSI. Furthermore, lumbar spine BMD, but not calcaneus OSI, was weakly but significantly associated with increased physical functioning score independently. In conclusion, it was suggested that physical activity may affect bone strength in lumbar spine and calcaneus and that FA IMT might be a significant determinant of bone strength in calcaneus, but not in lumbar spine, in healthy Japanese subjects.

Keywords ADL · Atherosclerosis · Bone mineral density · Osteoporosis · Quality of Life

S. Yamada · M. Inaba (✉) · H. Goto · M. Nagata · M. Ueda
K. Nakatuka · H. Tahara · H. Yokoyama · M. Emoto
T. Shoji · Y. Nishizawa
Department of Metabolism,
Endocrinology and Molecular Medicine,
Osaka City University Graduate School of Medicine,
1-4-3 Asahi-machi, Abeno-ku,
545-8585 Osaka, Japan
E-mail: inaba-m@med.osaka-cu.ac.jp
Tel.: +81-6-66453806
Fax: +81-6-66453808

Introduction

In healthy individuals, the relationship between atherosclerosis and bone mass has not been extensively studied. The hypothesis that reduced blood flow to the lower extremities may affect bone remodeling, resulting in a decrease in BMD, has been proposed [1]. Prospective community-based study showed that decreased vascular flow in the lower extremities may be associated with an increased rate of bone loss at the hip and calcaneus among relatively healthy older women [2]. Measurement of the far-wall intima-media thickness (IMT) of the common carotid artery (CA) and femoral artery (FA) by high-resolution ultrasonography has been established as a clinically useful index for identifying early-stage general and local atherosclerosis in lower extremities [3, 4, 5, 6, 7, 8, 9], since CA IMT is strongly correlated with the presence of coronary artery diseases [3, 4, 5, 6, 7, 8, 9], and FA IMT with local atherosclerosis [9].

Physical activity has been identified as having a favorable effect on bone status [10, 11] and atheroscle-

rosis [12]. We have reported that, in patients with rheumatoid arthritis, physical activity assessed by the modified Health Assessment Questionnaire (M-HAQ) score [13] correlated significantly in a positive manner with the osteo-sono assessment index (OSI) of the calcaneus by ultrasound [14]. Recently, the Medical Outcomes Study 36-item Short Form (SF-36), which is a self-administered questionnaire containing 36 items that, when scored, yield eight domains considering physical, cognitive, emotional, and social aspects [15, 16], has emerged as an valuable index to assess health-related quality of life (HRQL) [17].

This background prompted us to examine the influence of general and local atherosclerosis in lower extremities as reflected by CA IMT and FA IMT, respectively, on calcaneus OSI in comparison with lumbar spine BMD in healthy Japanese subjects. Furthermore, the modulatory effect of physical activity, as reflected by SF-36 score, was investigated on bone quality in calcaneus and lumbar spine, and arterial thickening.

Materials and methods

Subjects

Healthy subjects ($n=260$), 106 males and 154 females, were recruited from people who participated in a local health check program at the Osaka City University Hospital after written informed consent was obtained. The mean ages of healthy subjects were 51.4 ± 12.5 years. Exclusion criteria are the subjects who are known to be suffering from any major disease which might affect atherosclerosis and bone metabolism, such as hypertension, hyperlipidemia, diabetes mellitus, cerebral vascular accident impairing seriously activity of daily life (ADL), osteoporosis, and osteomalacia. The subjects who have been continuously taking medicines were also excluded from the present study.

Assessment of health-related quality of life (HRQL)

HRQL was assessed by means of SF-36 [15, 16]. The questionnaire consists of 36 items and measures three aspects of health: functional ability, well-being and overall health. These are quantified using eight multi-item domains (physical functioning, role-physical, bodily pain, general health, vitality, social functioning, role-emotional and mental health). The physical functioning domain assesses limitations in physical activities such as walking and climbing stairs. The role-physical and role-emotional domains measure problems with work or other daily activities as a result of physical health or emotional problems. Bodily pain assesses limitations resulting from pain; vitality measures energy and tiredness. The social functioning domain examines the effect of physical and emotional health on normal social activities, and mental health assesses happiness, nervousness, and depression. The general health perceptions domain evaluates the personal opinion of one's health compared with that of one's peers, as well as the expectation of changes in health. All domains are scored on a scale from 0 to 100, with 100 representing the best possible health state. Two summary scales (physical and mental component) can also be derived [16, 18].

The SF-36 has been validated for use to assess HRQL in osteoporotic patients [2, 19].

BMD measurement at lumbar spine

BMD was measured in the lumbar spine (L2–L4) in the anterior-posterior projection by dual-energy X-ray absorptiometry (DXA; QDR-4500A, Hologic Inc., Waltham, Mass., USA), essentially as previously described [20]. The precision of the measurement of lumbar spine BMD using DXA was less than 1.8%.

Quantitative ultrasound assessment of calcaneus

Quantitative ultrasound assessment of calcaneus was performed using an ultrasound system [Acoustic Osteo-Screener (AOS-100), Aloka Co. Ltd, Tokyo, Japan], as previously described [12, 14]. Briefly, the AOS-100 measures both speed of sound (SOS) and an attenuation-related parameter called the transmission index (TI). These measurements yield a derived parameter, the osteo sono-assessment index (OSI), which has been proposed to be an estimate of the elastic modulus of the calcaneus [22]. Precision of the OSI parameter was 2.2% [23].

Ultrasonographic examination of CA and FA IMT

Ultrasonographic examination of the CA and FA was performed in the supine position by high-resolution ultrasonography with a 10 MHz in-line Sectascanner (SSD 610 CL; Aloka), as previously described [12, 21, 24, 25, 26, 27]. To avoid inter-observer variability, all measurements were performed by the same examiner (H.Y.) who was unaware of subject characteristics. Briefly, CA and FA were scanned at the level of the bifurcation on both the right and left sides. IMT was measured in the far wall of the CA and FA at sites of the most advanced arterial thickening as diffuse and continuous projection with the greatest distance between the lumen-intimal interface and the media-adventitial interface but without atherosclerotic plaque, which was defined as localized lesions of thickness $\geqq 2.0$ mm, from digitized still images of the arteries during scanning [27, 28]. These interfaces were all manually traced on the same day to avoid possible variation during the study period and the mean value calculated as the mean of at least three still images obtained from the same section of the CA and FA [21, 24]. Reproducibility of the IMT measurement was acceptable as shown by coefficients of variation (CV) of

2.8% and 3.4% for CA IMT and FA IMT, respectively. These were calculated from the 40 measurements performed in 20 RA patients on two different occasions according to Bland and Altman [29] using the formula: $CV(\%) = 100(SD/\sqrt{2})/x$, where SD is the standard deviation of absolute differences between the two repeated measurements, and x is the pooled mean value.

Statistical analysis

Values are expressed as mean ± SD unless otherwise indicated. Statistical analysis was performed with the Stat View V system (Abacus Concepts, Berkeley, Calif., USA) for the Apple computer. The correlation coefficients were calculated by Pearson and Spearman Rank correlation analyses due to abnormal distribution of various clinical variables. *P*-values of < 0.05 were considered as statistically significant. Multiple regression analysis was performed to assess independent association with lumbar spine BMD and calcaneus OSI. *P*-values of < 0.05 were considered as statistically significant.

Results

Clinical variables, IMTs and bone density of healthy subjects

Clinical characteristics of healthy subjects ($n = 260$, M/F 106/154 enrolled in this cross-sectional study are shown in Table 1. CA and FA IMT were 0.603 ± 0.166 mm and 0.840 ± 0.396 mm, respectively. Lumbar spine BMD and calcaneus OSI were 0.918 ± 0.151 g/cm^2 and 2.69 ± 0.38×10^6, respectively. IMT at CA and FA and physical functioning score did not differ significantly between male and female, although lumbar spine BMD and calcaneus OSI were significantly lower in female than in male. As shown in Fig. 1, calcaneus OSI correlated significantly by Pearson correlation analysis in a positive manner with lumbar spine BMD in total subjects ($r = 0.551, P < 0.0001$).

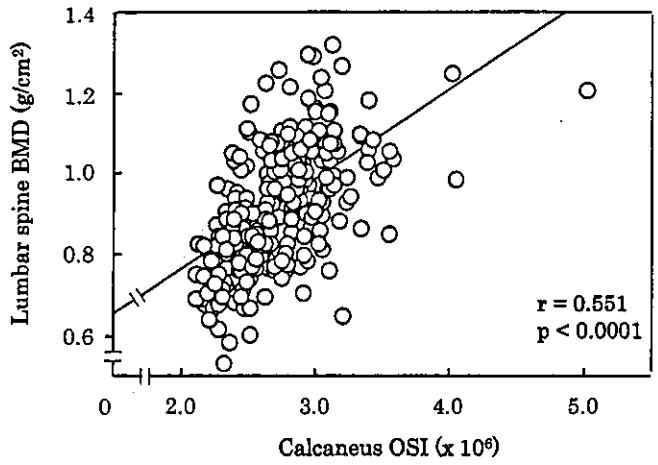

Fig. 1 Positive correlation between lumbar spine BMD and calcaneus OSI in 260 healthy Japanese subjects. A significant positive correlation was found between lumbar spine BMD and calcaneus OSI ($r = 0.551$, $P < 0.0001$) by Pearson analysis

Unadjusted domain scores of the eight subscales and adjusted domain scores of two summary scales of the SF-36 scores

Table 2 represents the HRQL scores assessed by SF-36. Adjusted domain scores of two summary scales were both around 50 points, confirming that the subjects enrolled in the present study have not been suffering from major health problems.

Correlation of lumbar spine BMD and calcaneus OSI with the SF-36 score

Among the eight subscales and two summary scales of the SF-36 scores, physical functioning emerged as the only factor which correlated significantly by Pearson correlation analysis in a positive manner with both lumbar spine BMD (Fig. 2) and calcaneus OSI (Fig. 3).

Table 1 Clinical characteristics of 260 healthy individuals enrolled in the present study. Data are expressed as mean ± SD, *BP* blood pressure, *LDL* low-density lipoprotein, *PF* physical functioning, *BMD* bone mineral density, *OSI* osteo-sono assessment index, *CA IMT* common artery intima-media thickness, *FA IMT* femoral artery intima-media thickness

	Total	Male	Female
Number	260	106	154
Age (years)	51.4 ± 12.5	47.4 ± 11.8	54.2 ± 12.2
Body weight (kg)	58.1 ± 11.3	67.1 ± 9.7	51.9 ± 7.5
Height (cm)	160.4 ± 9.6	169.4 ± 6.3	154.3 ± 6.1
Body mass index (kg/m^2)	22.5 ± 3.0	23.4 ± 2.7	21.8 ± 3.1
Postmenopausal	–	–	107
Smoking index	203.7 ± 371.4	461.2 ± 457.4	34.9 ± 140.6
Smoking habit	89	72	17
Systolic BP (mmHg)	123.9 ± 18.5	128.0 ± 15.3	121.1 ± 20.0
Diastolic BP (mmHg)	69.1 ± 10.6	71.2 ± 11.1	67.5 ± 10.0
LDL-cholesterol (mg/dl)	128.7 ± 32.4	121.0 ± 32.0	134.0 ± 31.7
PF score (SF-36)	90.9 ± 9.6	93.1 ± 8.2	89.5 ± 10.2
Lumbar 2–4 spine BMD (g/cm^2)	0.918 ± 0.151	0.979 ± 0.141	0.876 ± 0.145
Calcaneus OSI (×10^6)	2.69 ± 0.38	2.90 ± 0.39	2.55 ± 0.29
CA IMT (mm)	0.603 ± 0.166	0.600 ± 0.151	0.605 ± 0.176
FA IMT (mm)	0.840 ± 0.396	0.834 ± 0.398	0.845 ± 0.396

Table 2 Unadjusted domain scores of the eight subscales and two summary scales of the SF-36 scores. Data are expressed as mean ± SD

Scores in SF-36	
Physical functioning	91.0 ± 9.6
Role physical	91.2 ± 22.8
Bodily pain	76.9 ± 19.3
General health perceptions	64.4 ± 16.3
Vitality	64.4 ± 20.4
Social functioning	88.2 ± 17.6
Role emotional	87.0 ± 28.0
Mental health	73.2 ± 19.0
Summary scales in SF-36	
Physical components	52.4 ± 7.1
Mental components	48.3 ± 9.3

Correlations of lumbar spine BMD and calcaneus OSI with clinical variables including CA and FA IMT

Table 3 shows the summary of correlations of lumbar spine BMD and calcaneus OSI with clinical characteristics including IMTs at CA and FA by Spearman Rank correlation because of abnormal distributions of samples. Among the clinical variables included, gender, age, and BMI but not systolic blood pressure, were correlated significantly with both lumbar spine BMD and calcaneus OSI. Although FA IMT and physical functioning score of SF-36 correlated significantly with both lumbar spine BMD and calcaneus OSI, CA IMT did not correlate. Serum LDL cholesterol was negatively correlated with lumbar spine BMD but not calcaneus OSI.

Multiple regression analysis of factors independently associated with lumbar spine BMD and calcaneus OSI in male plus female subjects

Table 4 represents the results of multiple regression analysis of various clinical variables to evaluate their independent association with lumbar spine BMD and

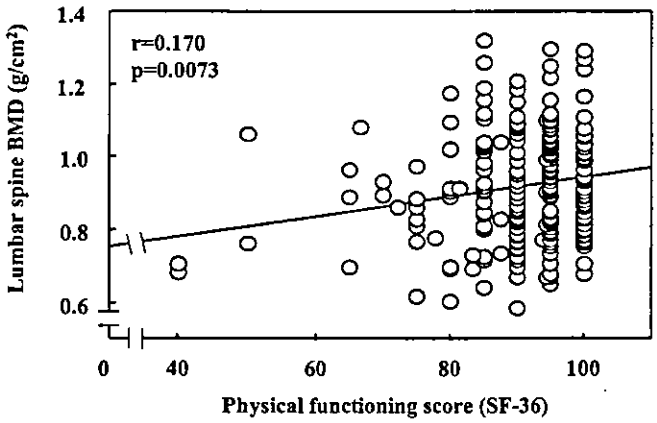

Fig. 2 Correlation of physical functioning score of SF-36 with lumbar spine BMD in 260 healthy Japanese subjects. A significant positive correlation was found between physical functioning and lumbar spine BMD ($r = 0.170$, $P = 0.0073$) by Pearson analysis

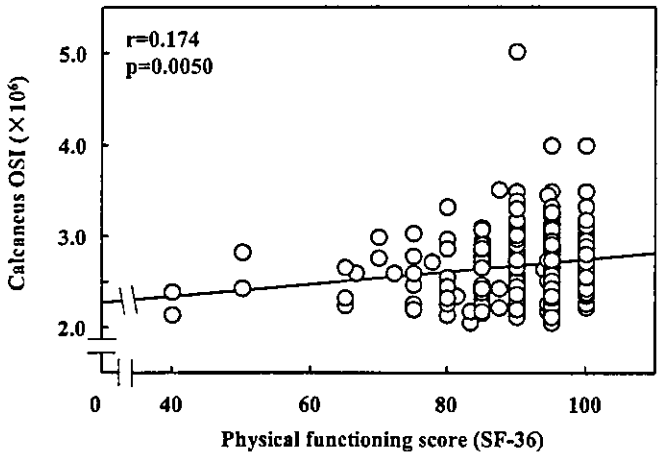

Fig. 3 Correlation of physical functioning score with calcaneus OSI in 260 healthy Japanese subjects. A significant positive correlation was found between physical functioning and calcaneus OSI ($r = 0.174$, $P = 0.0050$) by Pearson analysis

Table 3 Correlations of calcaneus OSI and lumbar spine BMD with clinical characteristics by Spearman rank correlation

Clinical variables	Lumbar spine BMD		Calcaneus OSI	
	ρ	P	ρ	P
Gender	−0.331	< 0.0001‡	−0.481	< 0.0001‡
Age (years)	−0.459	< 0.0001‡	−0.374	< 0.0001‡
Body mass index (kg/m²)	0.186	0.0038‡	0.411	< 0.0001‡
Systolic BP (mmHg)	−0.622	0.6868	0.075	0.2273
LDL-cholesterol (mg/dl)	−0.141	0.0266†	−0.071	0.2526
PF score (SF-36)	0.156	0.0147†	0.190	0.0024‡
CA IMT (mm)	−0.098	0.1225	−0.017	0.7867
FA IMT (mm)	−0.191	0.0027‡	−0.199	0.0014‡

‡$P < 0.01$, †$P < 0.05$

Table 4 Multiple regression analysis of factors independently associated with calcaneus OSI and lumbar spine BMD in male plus female. Values are standard regression coefficients (β). R^2 multiple coefficient of determination

Independent variables	Lumbar spine BMD		Calcaneus OSI	
	Model 1	Model 2	Model 1	Model 2
Gender	−0.038	−0.040	−0.273‡	−0.272‡
Age (years)	−0.470‡	−0.442‡	−0.312‡	−0.263‡
Body mass index (kg/m²)	0.233‡	0.235‡	0.312‡	0.301‡
Systolic BP (mmHg)	0.035	0.051	0.005	−0.007
Smoking index	0.025	0.023	0.042	0.077
LDL-cholesterol (mg/dl)	−0.034	−0.021	0.065	0.084
PF score (SF-36)	0.101§	0.102§	0.055	0.041
CA IMT (mm)	−0.037	–	0.017	–
FA IMT (mm)	–	−0.043	–	−0.117†
R^2	0.296‡	0.296‡	0.355‡	0.365‡

‡$P < 0.01$, †$P < 0.05$, §$P < 0.10$

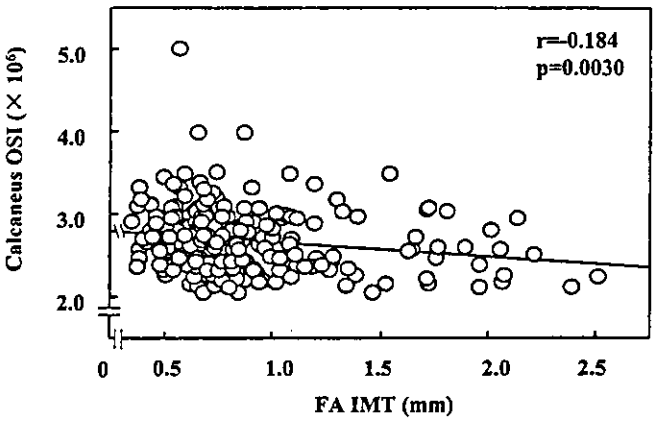

Fig. 4 Correlation of FA-IMT with calcaneus OSI in 260 healthy Japanese subjects. Negative correlation was found between FA-IMT and calcaneus OSI ($r=-0.184$, $P=0.0030$) by Pearson analysis

Table 5 Multiple regression analysis of factors independently associated with calcaneus OSI and lumbar spine BMD in female subjects. Values are standard regression coefficients (β). R^2 multiple coefficient of determination

Independent variables	Lumbar spine BMD		Calcaneus OSI	
	Model 1	Model 2	Model 1	Model 2
Age (years)	−0.203	−0.190	−0.170	−0.069
Body mass index (kg/m^2)	0.196†	0.190†	0.370‡	0.351‡
Menopause	−0.418‡	−0.422‡	−0.377‡	−0.389‡
Systolic BP (mmHg)	0.089	0.086	−0.001	−0.017
Smoking index	−0.068	−0.066	0.091	0.116
LDL-cholesterol (mg/dl)	0.009	0.008	0.092	0.103
PF score (SF-36)	0.084	0.088	0.056	0.059
CA IMT (mm)	−0.012	–	0.040	–
FA IMT (mm)	–	−0.021	–	−0.139§
R^2	0.319‡	0.320‡	0.338‡	0.351‡

‡$P<0.01$, †$P<0.05$, §$P<0.10$

calcaneus OSI. In model 1, which included gender, age, BMI, systolic BP, smoking index, serum LDL cholesterol, physical functioning score of SF-36 and CA IMT, only age and BMI were independent factors significantly associated with lumbar spine BMD. There was a tendency toward higher physical functioning score in those with higher lumbar BMD. In case of calcaneus OSI, gender, in addition to age and BMI, emerged as the independently associated factor. CA IMT failed to be significantly associated with both lumbar spine BMD and calcaneus OSI. In model 2, which included FA IMT in the place of CA IMT, FA IMT, of great interest, emerged as an independent factor significantly associated with calcaneus OSI, but not lumbar spine BMD (Table 4 and Fig. 4).

Multiple regression analysis of factors independently associated with lumbar spine BMD and calcaneus OSI in female subjects

Table 5 represents the results of multiple regression analysis when the subjects were restricted to females only. The results were essentially the same, indicating the tendency towards independent association of FA IMT selectively with calcaneus OSI but not with lumbar spine BMD, although the association did not reach statistical significance ($P=0.0787$). It was reasonable that menopause was negatively associated with both lumbar spine BMD and calcaneus OSI.

Discussion

Since the physical functioning domain of SF-36 scores assesses limitations in physical activities such as walking and climbing stairs, it is reasonable that it showed a significant and positive correlation with lumbar spine BMD and calcaneus OSI, since a large body of literature supports the positive impact of physical activity on bone mass, particularly in weight-bearing bones such as lumbar spine and calcaneus [30, 31, 32, 33, 34, 35, 36, 37]. By multiple regression analysis, physical functioning score showed a tendency of independently associating with lumbar spine BMD. However, it did not associate with calcaneus OSI, in spite of the positive impact on bone mass. One possibility for the lack of its positive associations with calcaneus OSI might be ascribed to the inclusion criteria that the subjects enrolled in the present study were restricted to those in good health and were eager to join the health programs spontaneously and thus that the distribution of HRQL scores in the subjects fell within the narrower ranges. Alternatively, it might be explained by less precision of calcaneus OSI compared to that of lumbar spine BMD. When we extended the ranges of ADL of the subjects to include patients with early rheumatoid arthritis, we found a significant correlation of ADL score assessed using a self-administered questionnaire modified from the Stanford Health Assessment Questionnaire, named MHAQ [13] with calcaneus OSI [14].

The most important finding in the present study is that FA IMT emerged as an independent factor that significantly associated with calcaneus OSI but not with lumbar spine BMD (Table 4). When the subjects were restricted to female patients, FA IMT was independently associated with calcaneus OSI, but not with lumbar spine BMD, although the association was not significant due probably to smaller numbers of subjects because of higher β-value than that in whole subjects (Table 5).

We have previously observed a significant correlation between peak wave velocity, an index of atherosclerosis, and bone mineral content (BMC) in the paretic lower limbs in hemiparetic patients [37]. Although bone loss and arterial disease of the lower limbs certainly shares common risk factors, such as tobacco

consumption and sedentary life style, bone loss in the affected lower limbs seems to be related with a direct local effect of atherosclerosis and not with associated general risk factor since the more ischemic atherosclerosis limb also showed greater bone loss [38]. These considerations are also supported from the present study demonstrating that CA IMT, in contrast to FA IMT, failed to be independently associated with calcaneus OSI (Table 4). The reason for greater bone loss in the less-perfused lower limbs is explained by several mechanisms. Since a correlation exists between intraosseous blood flow and bone remodeling in humans [39], it is conceivable that reduced intraosseous blood flow secondary to arterial disease induced osteopenia by suppressing bone formation and stimulating bone resorption. In fact, it was demonstrated that atherosclerotic lesions in the intraosseous arterioles were indentical to those in the cutaneous, muscular or myocardial vessels [40]. It is possible that hindlimb unloading-induced decreases in blood flow and increase in shear stress alter vascular endothelial cell release of nitric oxide (NO) and prostaglandin I_2 (PGI_2), which could subsequently modify the focal balance between osteoblast and osteoclast activity [41]. These data may suggest that enhanced local atherosclerosis, as reflected by increased FA IMT, may facilitate local bone loss by reducing intraosseous blood flow even in normal population of Japanese people, resulting in accelerated bone loss. The clinical significance of the present study is the association of local blood flow in lower extremities with reduction in calcaneus OSI. Therefore, these data may suggest that we should be careful of bone loss in calcaneus in those whose blood flow in the lower extremities may be impaired.

The limitation of the present study is that the multiple regression model explained only 35.5–36.5% of the variance of calcaneus OSI. This may indicate the presence of other factors affecting calcaneus OSI, that were not included in the models. Furthermore, due to small numbers of subjects, analyses were performed in subjects including male and female, although FA IMT emerged as a factor independently associated with calcaneus OSI even after adjustment for gender in the multiple regression analysis. Another limitation of the present study is that we have no direct histopathological demonstration that increased IMT is due to atherosclerosis. The arterial thickening might have been due to another, non-atherosclerotic arteriopathy. However, IMT measurement is still useful in that IMT is strongly correlated with the presence of coronary artery diseases.

In summary, it was suggested that the beneficial influence of physical activity on bone status as measured by calcaneus OSI and lumbar spine BMI was evident in healthy Japanese population. Furthermore, as reflected by the importance of FA IMT in the maintenance of calcaneal ultrasonographic values, but not lumbar spine BMD, it was strongly suggested that the importance of local blood flow in the maintenance of bone quality even in apparently healthy Japanese population.

References

1. Vogt MT, Cauley JA, Kuller LH et al. (1997) Bone mineral density and blood flow to the lower extremities: the study of osteoporotic fractures. J Bone Miner Res 12:283–289
2. Adachi JD, Loannidis G, Berger C et al. (2001) Canadian Multicentre Osteoporosis Study (CaMos) Research Group. The influence of osteoporotic fractures on health-related quality of life in community-dwelling men and women across Canada. Osteoporos Int 12:903–908
3. Salonen R, Salonen JT (1990) Progression of carotid atherosclerosis and its determinants: a population-based ultrasonography study. Atherosclerosis 81:33–40
4. Kawamori R, Yamasaki Y, Matsushima H et al. (1992) Prevalence of carotid atherosclerosis in diabetic patients: ultrasound high-resolution B-mode imaging on carotid arteries. Diabetes Care 15:1290–1294
5. Yamasaki Y, Kawamori R, Matsushima H et al. (1994) Atherosclerosis in carotid artery of young IDDM patients monitored by ultrasound high-resolution B-mode imaging. Diabetes 43:634–639
6. Wofford J, Kahl F, Howard G et al. (1991) Relation of extent of extracranial carotid artery atherosclerosis as measured by B-mode ultrasound to the extent of coronary atherosclerosis. Arterioscler Thromb 11:1786–1794
7. Lekakis JP, Papamichael CM, Cimponeriu AT et al. (2000) Atherosclerotic changes of extracoronary arteries are associated with the extent of coronary atherosclerosis. Am J Cardiol 85:949–952
8. Simons PC, Algra A, Bots ML et al. (1999) Common carotid intima-media thickness and arterial stiffness: indicators of cardiovasucular risk in high-risk patients. The SMART Study (Second Manifestation of ARTerial disease). Circulation 100:951–957
9. Taniwaki H, Shoji T, Emoto M et al. (2001) Femoral artery wall thickness and stiffness in evaluation of peripheral vascular disease in type 2 diabetes mellitus. Atherosclerosis 158:207–214
10. Neville CE, Murray LJ, Boreham CA et al. (2002) Relationship between physical activity and bone mineral status in young adults: the Northern Ireland Young Hearts Projects. Bone 30:792–798
11. Lehtonen-Veromaa M, Mottonenn T, Nuotio I et al. (2000) Influence of physical activity on ultrasound and dual-energy X-ray absorptiometry bone measurements in peripubertal girls: a cross-sectional study. Calcif Tissue Int 66:248–254
12. Kumeda Y, Inaba M, Goto H et al. (2002) Increased thickness of the arterial intima-media detected by ultrasonography in patients with rheumatoid arthritis. Arthr Rheum 46:1489–1497
13. Pincus T, Summey JA, Soraci SA Jr et al. (1983) Assessment of patient satisfaction in activities of daily living using a modified Stanford Health Assessment Questionnaire. Arthr Rheum 26:1346–1353
14. Inaba M, Nagata M, Goto H et al. (2003) Preferential reductions of paraarticular trabecular bone component in ultradistal radius and of calcaneus ultrasonography in early-stage rheumatoid arthritis. Osteoporos Int 14:683–687
15. Ware JE (1993) SF-36 Health Survey Manual and Interpretation Guide. The Health Institute, New England Medical Center, Boston, Mass.
16. Fukuhara S, Bito S, Green J et al. (1998) Translation, adaptation, and validation of the SF-36 Health Survey for use in Japan. J Clin Epidemiol 51:1037–1044
17. Fukuhara S, Ware J E, Kosinski M et al. (1998) Psychometric and clinical tests of validity of the Japanese SF-36 Health Survey for use in Japan. J Clin Epidemiol 51:1045–1053
18. Ware JE, Kosinski M, Keller SD (1994) SF-36 Physical and Mental Health Summary Scales: a user's manual. The Health Institute, New England Medical Centre, Boston, Mass.
19. Tosteson AN, Gabriel SE, Grove MR et al. (2001) Impact of hip and vertebral fractures on quality-adjusted life years. Osteoporos Int 12:1042–1049

20. Inaba M, Nishizawa Y, Mita K et al. (1999) Poor glycemic control impairs the response of biochemical parameters of bone formation and resorption to exogenous 1,25-dihydroxyvitamin D_3 in patients with type 2 diabetes. Osteoporos Int 9:525–531
21. Nagata-Sakurai M, Inaba M, Goto H et al. (2003) Importance of inflammation and bone resorption in an increase of arterial intima-media thickness (IMT) in patients with rheumatoid arthritis (RA). Arthr Rheum 48:3061–3067
22. Cheng S, Njeh CF, Fan B et al. (2002) Influence of region of interest and bone size on calcaneus BMD: implications for the accuracy of quantitative ultrasound assessments at the calcaneus. Br J Radiol 75:59–68
23. Tsuda-Futami E, Hans D, Njeh CF et al. (1999) An evaluation of a new gel-coupled ultrasound device for the quantitative assessment of bone. Br J Radiol 72:691–700
24. Nagasaki T, Inaba M, Henmi Y et al. (2003) Decrease in carotid intima-media thickness in hypothyroid patients after normalization of thyroid function. Clin Endocrinol 59:607–612
25. Kawagishi T, Nishizawa Y, Konishi T et al. (1995) High-resolution B-mode ultrasonography in evaluation of atherosclerosis in uremia. Kidney Int 48:820–826
26. Hirai T, Sasayama S, Kawasaki T et al. (1989) Stiffness of systemic arteries in patients with myocardial infarction: a noninvasive method to predict severity of atherosclerosis. Circulation 80:78–86
27. Hosoi M, Nishizawa Y, Kogawa K et al. (1996) Angiotensin-converting enzyme gene polymorphism is associated with carotid arterial wall thickness in non-insulin-dependent diabetes patients. Circulation 94:704–707
28. Poli A, Tremoli E, Colombo A et al. (1988) Ultrasonographic measurement of the common carotid artery wall thickness in hypercholesterolemic patients: a new model for the quantitation and follow-up of preclinical atherosclerosis in living human subjects. Atherosclerosis 70:253–261
29. Bland JM, Altman DG (1986) Statistical methods for assessing agreement between two methods of clinical measurement. Lancet 1:307–310
30. Friedlander AL, Genant HK, Sadowsky S et al. (1995) A two-year program of aerobics and weight training enhances bone mineral density of young women. J Bone Miner Res 10:574–585
31. Shigematsu T, Miyamoto A, Mukai C et al. (1997) Changes in bone and calcium metabolism with space flight. Osteoporos Int 7:S63–7
32. Boot AM, de Ridder MAJ, Pols HA et al. (1997) Bone mineral density in children and adolescents: relation to puberty, calcium intake, and physical activity. J Clin Endocrinol Metab 82:57–62
33. Damilakis J, Perisinakis K, Kontakis et al. (1999) Effect of lifetime occupational physical activity on indices of bone mineral status in healthy postmenopausal women. Calcif Tissue Int 64:112–116
34. Daly RM, Rich PA, Klein R (1997) Influence of high impact loading on ultrasound bone measurements in children: a cross-sectional study. Calcif Tissue Int 60:401–404
35. Lappe JM, Recker RR, Weidenbusch D (1998) Influence of activity level on patellar ultrasound transmission velocity in children. Osteoporos Int 8:39–46
36. Hoshino H, Kushida K, Yamazaki K et al. (1996) Effect of physical activity as a caddie on ultrasound measurements of the os calcis: a cross-sectional comparison. J Bone Miner Res 11:412–418
37. Okabe R, Inaba M, Sakai S et al. (2004) Enhanced atherosclerosis in paretic lower in the patients with hemiparesis. Clin Sci (Lond) 166:613–618
38. Laroche M, Pouilles JM, Ribot C et al. (1994) Comparison of the bone mineral content of the lower limbs in men with ischemic atherosclerotic disease. Clin Rheum 13:611–614
39. Laroche M, Barbier A, Ludot I et al. (1996) Effect of ovariectmy on intraosseous vascularization and bone remodelling in rats: action of tiludronate. Osteoporos Int 6:127–129
40. Reeve J, Arlot M, Wootton R et al. (1988) Skeletal blood flow, iliac histomorphometry and strontium kinetics in osteoporosis: a relationship between blood flow and corrected apposition rate. J Clin Endcrinol Metab 66:1124–1131
41. Burkhardt R, Barti R, Frisch B et al. (1984) The structural relationship of bone forming and endothelial cells of the bone marrow. In: Bone circulation. Williams and Wilkins, Baltimore, pp 2–14

The centrosomal protein Lats2 is a phosphorylation target of Aurora-A kinase

Shingo Toji[1,†], Norikazu Yabuta[2,†], Toshiya Hosomi[2], Souichi Nishihara[2], Toshiko Kobayashi[1], Susumu Suzuki[1], Katsuyuki Tamai[1] and Hiroshi Nojima[2,*]

[1]*Ina Laboratories, MBL Co. Ltd, Ina, Nagano 396-0002, Japan*
[2]*Department of Molecular Genetics, Research Institute for Microbial Diseases, Osaka University, 3-1 Yamadaoka, Suita City, Osaka 565-0871, Japan*

Human Lats2, a novel serine/threonine kinase, is a member of the Lats kinase family that includes the *Drosophila* tumour suppressor *lats/warts*. Lats1, a counterpart of Lats2, is phosphorylated in mitosis and localized to the mitotic apparatus. However, the regulation, function and intracellular distribution of Lats2 remain unclear. Here, we show that Lats2 is a novel phosphorylation target of Aurora-A kinase. We first showed that the phosphorylated residue of Lats2 is S83 *in vitro*. Antibody that recognizes this phosphorylated S83 indicated that the phosphorylation also occurs *in vivo*. We found that Lats2 transiently interacts with Aurora-A, and that Lats2 and Aurora-A co-localize at the centrosomes during the cell cycle. Furthermore, we showed that the inhibition of Aurora-A-induced phosphorylation of S83 on Lats2 partially perturbed its centrosomal localization. On the basis of these observations, we conclude that S83 of Lats2 is a phosphorylation target of Aurora-A and this phosphorylation plays a role of the centrosomal localization of Lats2.

Introduction

The onset and exit of mitosis are tightly regulated by the phosphorylation and dephosphorylation of numerous proteins. These mitotic phosphorylations are carried out by various mitotic serine/threonine kinases such as Cdk, Polo, NIMA and Aurora (reviewed in Nigg 2001). Members of these kinase families are highly conserved from yeast to human and participate in centrosome maturation and separation, spindle assembly, nuclear envelope breakdown, chromosome condensation and cytokinesis. According to recent studies in yeast and *Drosophila melanogaster*, mutations in these kinases can lead to phenotypes that are characteristic of defects in mitosis, including monopolar spindles, unequally separated bipolar spindles and failure in cytokinesis. This suggests that inaccurate controls of mitotic processes can lead to aneuploidy or genetic instability, finally causing tumour formation or apoptosis (Nigg 2001). Therefore, to understand oncogenesis and tumour progression, it is crucial to define the signalling pathways of these mitotic kinases.

The *Drosophila* Aurora gene, which is highly homologous to *Saccharomyces cerevisiae* IPL1, was identified in a search for the gene that regulates the formation of a functional centrosome and mitotic spindle (reviewed in Bischoff & Plowman 1999; Giet & Prigent 1999). Amorphic alleles of aurora result in pupal lethality and in mitotic arrest in which the condensed chromosomes are arranged on circular monopolar spindles. The loss of function of the Aurora kinase causes failures in centrosome separation and bipolar spindle formation (Glover *et al.* 1995). In mammals, the Aurora kinase family consists of at least three members, including Aurora-A, Aurora-B and Aurora-C (Adams *et al.* 2001; Nigg 2001). Aurora-A is prominent both at the centrosomes and in the nucleus of G_2 phase cells and at the half-spindle (a zone between the kinetochore and the spindle pole) in metaphase and telophase cells (Crosio *et al.* 2002; Hirota *et al.* 2003).

†The first two authors contributed equally to this work.
Communicated by: Eisuke Nishida
**Correspondence*: E-mail: hnjm2606@biken.osaka-u.ac.jp

DOI: 10.1111/j.1356-9597.2004.00732.x

Therefore, Aurora-A is considered to be involved in centrosome maturation and mitotic spindle assembly (Dutertre *et al.* 2002; Blagden & Glover 2003). Aurora-B is prominent in the nucleus during interphase, at the midzone during anaphase and in post-mitotic bridges during telophase, and is considered to be involved in chromosomal events and cytokinesis (Adams *et al.* 2001). Aurora-C is localized to the centrosome during the later stages of mitosis but its function is not yet clear (Kimura *et al.* 1999). Therefore, these Aurora kinase homologues are implicated in mitotic regulation including centrosome duplication, centrosome maturation, chromosome segregation and cytokinesis (reviewed in Dutertre *et al.* 2002; Blagden & Glover 2003).

Human Aurora-A is reported to be located on chromosome 20q13, a region that is frequently amplified in breast cancers and in diverse cancer cell lines. Over-expression of Aurora-A leads to abnomal centrosome amplification, chromosomal instability and transformation of NIH3T3 cells (Bischoff *et al.* 1998; Zhou *et al.* 1998). In $p53^{-/-}$ cells, over-expression of Aurora-A also causes extra centrosomes through defects in cytokinesis and consequent tetraploidization (Meraldi *et al.* 2002). This effect is blocked by p53, which directly binds and inhibits Aurora-A (Chen *et al.* 2002). Moreover, in primary cultures of mouse embryo fibroblasts, over-expression of Aurora-A inaccurately enters anaphase despite defective spindle formation, indicating that the elevated Aurora-A expression overrides the mitotic spindle assembly checkpoint (Anand *et al.* 2003). Recently, some attractive studies on the novel phosphorylation targets of human Aurora-A have been reported. One of the reports showed that human Aurora-A can phosphorylate PP1, a protein phosphatase type 1 and phosphorylations of PP1 by Aurora-A inhibit its phosphatase activity in HeLa cells (Katayama *et al.* 2001). Moreover, TPX2, a prominent component of the spindle apparatus, has been shown to be required for recruiting Aurora-A to spindle microtubeles in HeLa cells and to be the likely regulator of Aurora-A activity at mitotic spindle in *Xenopus* eggs, albeit the biological function of phosphorylation of TPX2 by Aurora-A remains unclear (Kufer *et al.* 2002; Eyers *et al.* 2003; Tsai *et al.* 2003). TACC3, a human homologue of the centrosomally associated protein D-TACC, has also been shown to be phosphorylated by Aurora-A (Giet *et al.* 2002). Phosphorylation of D-TACC by Aurora-A is probable because the recruitment of D-TACC to the centrosome requires the phosphorylation of additional centrosomal substrates (Blagden & Glover 2003). These observations suggest that Aurora-A protein is crucial for genomic stability and the maintenance of the cell cycle progression in mammalian cells.

Mammalian Lats2, a novel serine/threonine kinase, is a member of Lats kinase family to which the *Drosophila* tumour suppressor *lats/warts* also belongs (Yabuta *et al.* 2000). Mutation of the *lats* gene leads to dramatic over-proliferation of phenotypes and diverse developmental defects in *Drosophila* mosaic animals and homozygous mutants (Justice *et al.* 1995; Xu *et al.* 1995). Similar to the *Drosophila* mutants, mice deficient in *LATS1* gene, a counterpart of *LATS2*, have been shown to develop soft-tissue sarcomas and ovarian stromal cell tumours (St. John *et al.* 1999). However, no reports on mice deficient in the *LATS2* gene have been shown.

Structural comparisons between mammalian Lats1 and Lats2 have revealed that the overall sequence similarity in the N-terminus between these proteins is much lower than in the kinase domain, except for two stretches of highly conserved sequence (Hori *et al.* 2000; Yabuta *et al.* 2000; Li *et al.* 2003). Therefore, the structural diversity or different modifications of the N-terminus between Lats1 and Lats2 are important to execute their independent functions during cell cycle. Enhanced expression of *LATS1* in human tumour cell lines caused cell cycle arrest at G_2/M through inhibition of Cdc2 kinase activity or induced apoptosis by up-regulating the level of pro-apoptotic proteins such as Bax or Caspase-3 (Yang *et al.* 2001; Xia *et al.* 2002). Moreover, Lats1 is phosphorylated in early prophase to function as a negative regulator of Cdc2 kinase by interacting with Cdc2 during mitosis (Tao *et al.* 1999) and is localized to the mitotic apparatus (Nishiyama *et al.* 1999; Hirota *et al.* 2000). Human *LATS2* is located at chromosome 13q11-12, in which a loss of heterozygosity has been frequently observed in many primary cancers (Yabuta *et al.* 2000). Over-expression of human Lats2/Kpm in HeLa cells has also shown to cause G_2/M arrest through inhibition of Cdc2 kinase activity and to induce apoptosis (Hori *et al.* 2000; Kamikubo *et al.* 2003), whereas over-expression of mouse Lats2 in *v-ras*-transformed NIH3T3 cells has shown to inhibit G_1/S transition through down-regulation of Cyclin E/Cdk2 kinase activity and to suppress tumorigenicity of NIH3T3/*v-ras* cells (Li *et al.* 2003). These observations suggest that Lats kinases act as tumour suppressors by inhibition of cell cycle progression or apoptosis. Although Lats1 was recently found to be phosphorylated by Cdc2 (Morisaki *et al.* 2002), the kinase that phosphorylates Lats2 has not yet been identified.

In this study, we show that Lats2 is phosphorylated by human Aurora-A kinase and that Lats2 and Aurora-A co-localize to the centrosome during the cell cycle. We also show that the Aurora-A-induced phosphorylation on Lats2 plays a role in its centrosomal localization.

Results

Lats2 is phosphorylated during the cell cycle

Lats2 has been reported to be phosphorylated in the M phase (Hori *et al.* 2000). We therefore examined, here, the phosphorylation state of Lats2 during the cell cycle by arresting HeLa cells at the G_1/S phase by using the thymidine-aphidicoline double block method (Fig. 1A). Cells were harvested at the indicated times after the blocks had been removed and analysed by Western blotting with an anti-human Lats2 monoclonal antibody (3D10) (Yabuta *et al.* 2000). In synchronized cells, we observed that Lats2 migrated as two bands, one that migrated slowly and another that migrated more quickly. The slowly migrating band was particularly prominent in lysates of cells that had progressed to the M phase (8 h after release from the G_1/S phase). We also observed this band shift in the lysates of mitotic HeLa cells that had been treated by the microtubule-depolymerizing agent

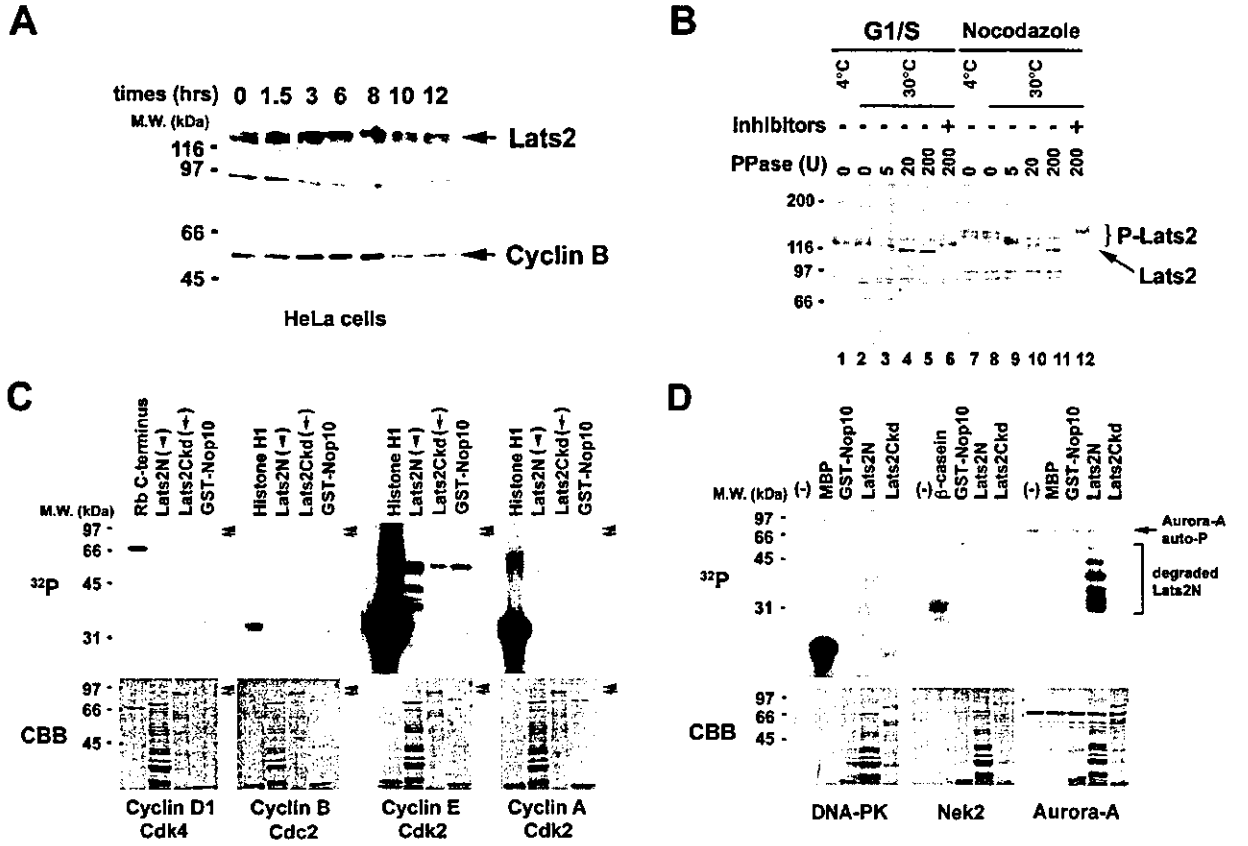

Figure 1 The phosphorylation of Lats2 is dependent on the cell cycle phase. (A) HeLa cells were arrested in the G_1/S phase by the thymidine-aphidicoline double block method. Cells were released from the block by replacing the medium with fresh medium without drugs. Thirty micrograms of each extract prepared at the indicated time (h) after the release were analysed by Western blotting for Lats2 or Cyclin B. (B) HeLa cells were arrested in the G_1/S phase as time = 0 in A (left side) or the M phase by nocodazole-treatment (right side). The nuclear extract (Yabuta *et al.*, 2000) from each cell was incubated at 4 °C or 30 °C with the indicated concentrations (units) of lambda protein phosphatase (New England Biolabs) in the absence (–) or presence (+) of phosphatase inhibitors. These extracts were analysed by Western blotting with the 3D10 antibody. (C) Cyclin D1/Cdk4, Cyclin B/Cdc2, Cyclin E/Cdk2 and Cyclin A/Cdk2 kinase complexes purified from Sf-9 insect cells were used in *in vitro* kinase reactions. The substrates used were Rb C-terminus (for only Cyclin D1/Cdk4), Histone H1, GST-Lats2N (79–621), GST-Lats2Ckd (622–1088, kinase dead) or GST-Nop10 (as a negative control). These proteins were resolved by SDS–PAGE and ^{32}P-labelled proteins were visualized by autoradiography. The arrowheads and arrows indicate the locations of the GST-Lats2N (*c.* 96 kDa) and GST-Lats2C kDa (*c.* 86 kDa) proteins, respectively. Coomassie Brilliant Blue (CBB) staining shows a loading control (bottom panels). (D) An *in vitro* kinase reaction was performed with three different kinases and two Lats2 substrates. The kinases were GST-DNA-PK, GST-Nek2 and GST-Aurora-A. The substrates were GST-Lats2N (79–621) and GST-Lats2Ckd (622–1088, kinase dead). As a negative control substrate, GST-Nop10 was used. The proteins were resolved by SDS–PAGE and ^{32}P-labelled proteins were visualized by autoradiography. CBB staining shows a loading control (bottom panels).

nocodazole (Fig. 1B, lanes 7 and 8). To examine whether this band shift is due to phosphorylation of Lats2, nocozazole-treated HeLa cell lysates were incubated with various concentrations of lambda-protein phosphatase (Fig. 1B, lanes 9–11). The slowly migrating Lats2 band was converted into the fast-migrating band after the phosphatase treatment in a dose-dependent manner. This conversion was completely blocked by the addition of phosphatase inhibitors (Fig. 1B, lane 12), indicating that Lats2 is indeed phosphorylated at the M phase, in which nocodazole-treated cells are arrested by the spindle assembly checkpoint. Interestingly, we observed that the band corresponding to the Lats2 protein in the G_1/S-arrested cell lysates (the same sample as cell lysate of 0 h in Fig. 1A) was also converted by the phosphatase treatment into the fast-migrating band, which showed a similar mobility as the band in lane 11 of Fig. 1(B) (Fig. 1B, lanes 1–5). This conversion was also completely blocked by the addition of phosphatase inhibitors. These results indicate that Lats2 is phosphorylated not only at the M phase but also at the G_1/S phase. This G_1/S-phosphorylated band was also observed during interphase (Fig. 1A; 0, 1.5, 3, 10 and 12 h), indicating that Lats2 is phosphorylated during interphase. Therefore, these findings suggest that Lats2 is regulated by at least two distinct phosphorylation events during the cell cycle.

Lats2 is phosphorylated by Aurora-A *in vitro*

This cell cycle-dependent phosphorylation of Lats2 suggests that the regulation of Lats2 may be directly involved in cell cycle regulation. We wondered, therefore, whether the cell cycle-dependent phosphorylation of Lats2 could be mediated by the Cyclin/Cdk kinases. To test this notion, we performed *in vitro* kinase assays with four classes of Cyclin/Cdk kinases, namely, Cyclin D1/Cdk4, Cyclin B/Cdc2, Cyclin E/Cdk2 and Cyclin A/Cdk2, which act in G_1, G_2/M, G_1/S and S, respectively (Kitagawa *et al.* 1996). The substrates used were two truncated forms of glutathione-*S*-transferase (GST)-fused Lats2, namely, Lats2N (amino acids 79–621) and Lats2Ckd (amino acids 622–1088) (Fig. 2A) because full-length Lats2 was too unstable for recovery. We did not prepare the 1–78 amino acids region of Lats2 for a substrate of Cdk kinases because there is no consensus sequence of the Cdk phosphorylation site (S/T-P-X-R/K) (Kitagawa *et al.* 1996) in this region. GST-Lats2Ckd, which is defective in kinase activity due to the substitution of the catalytically essential lysine 687 residue with methionine (data not shown), was used rather than the intact Lats2C protein to prevent the autophosphorylation of Lats2C. As shown in Fig. 1(C), Cyclin D1/Cdk4 and Cyclin B/Cdc2 kinases could not phosphorylate either of the GST-Lats2 constructs, although these Cyclin/Cdk kinases could phosphorylate the substrates used as positive controls (Rb C-terminus or Histone H1). Although Cyclin E/Cdk2 and Cyclin A/Cdk2 appeared to slightly phosphorylate the degraded products of Lats2N, these may not be the major phosphorylation events to which Lats2 is subjected during the cell cycle because they are of similar intensity as the phosphorylation of the negative control substrate Nop10, which is a protein involved in the pseudouridylation of pre-rRNAs (Henras *et al.* 1998). These results suggest that the cell cycle-dependent phosphorylation of Lats2 is due to kinase(s) other than the Cyclin/Cdk kinases. In particular, it appears that the mitosis-dependent phosphorylation of Lats2 is not due to Cyclin B/Cdc2 kinase, which functions during mitosis.

As the kinase that phosphorylates Lats2 is not known, we searched for candidates with the *in vitro* kinase assay. When we tested DNA-PK (Kim *et al.* 1999), Nek2 (Fry *et al.* 1995) and Aurora-A, we found that only Aurora-A could phosphorylate Lats2N efficiently *in vitro* (Fig. 1D). Aurora A could not, however, phosphorylate GST-Lats2Ckd. Aurora-A is reported to be a centrosomal protein kinase whose kinase activities are regulated in a cell cycle-dependent manner (Nigg 2001) and peak at the G_2/M phase (Bischoff *et al.* 1998; Farruggio *et al.* 1999; Hirota *et al.* 2003).

Aurora-A kinase phosphorylates the serine 83 of Lats2 *in vitro*

To determine more specifically the region of Lats2 that is phosphorylated by Aurora-A, we produced several deletion mutants of Lats2 as GST-fusion proteins (Fig. 2A) and used them as substrates in the *in vitro* kinase assay. As shown in Fig. 2(B), GST-Lats2 proteins containing amino acids 1–118, 79–118, 79–151, 79–257 and 79–621 were readily phosphorylated by Aurora-A, whereas the Lats2 proteins consisting of amino acids 1–78 and 113–151 were very poorly phosphorylated. This suggests that Aurora-A directly phosphorylates the amino acid 79–118 region of Lats2. To further map the Aurora-A phosphorylation site(s) on Lats2, we mutated serine 83 (S83), S91, threonine 93 (T93) or S94 in GST-79-118 to cysteine (S83C), cysteine (S91C), aspartic acid (T93D) or alanine (S94A), respectively. *In vitro* kinase assays with Aurora-A were performed with these mutated sequences. A loading control experiment with Coomassie Blue staining showed that an equal amount of each protein had been applied (Fig. 2C, right panel). Whereas phosphorylation of the S91C, T93D or S94A mutants was not significantly altered, the phosphorylation of the S83C mutant was remarkably diminished (Fig. 2C,

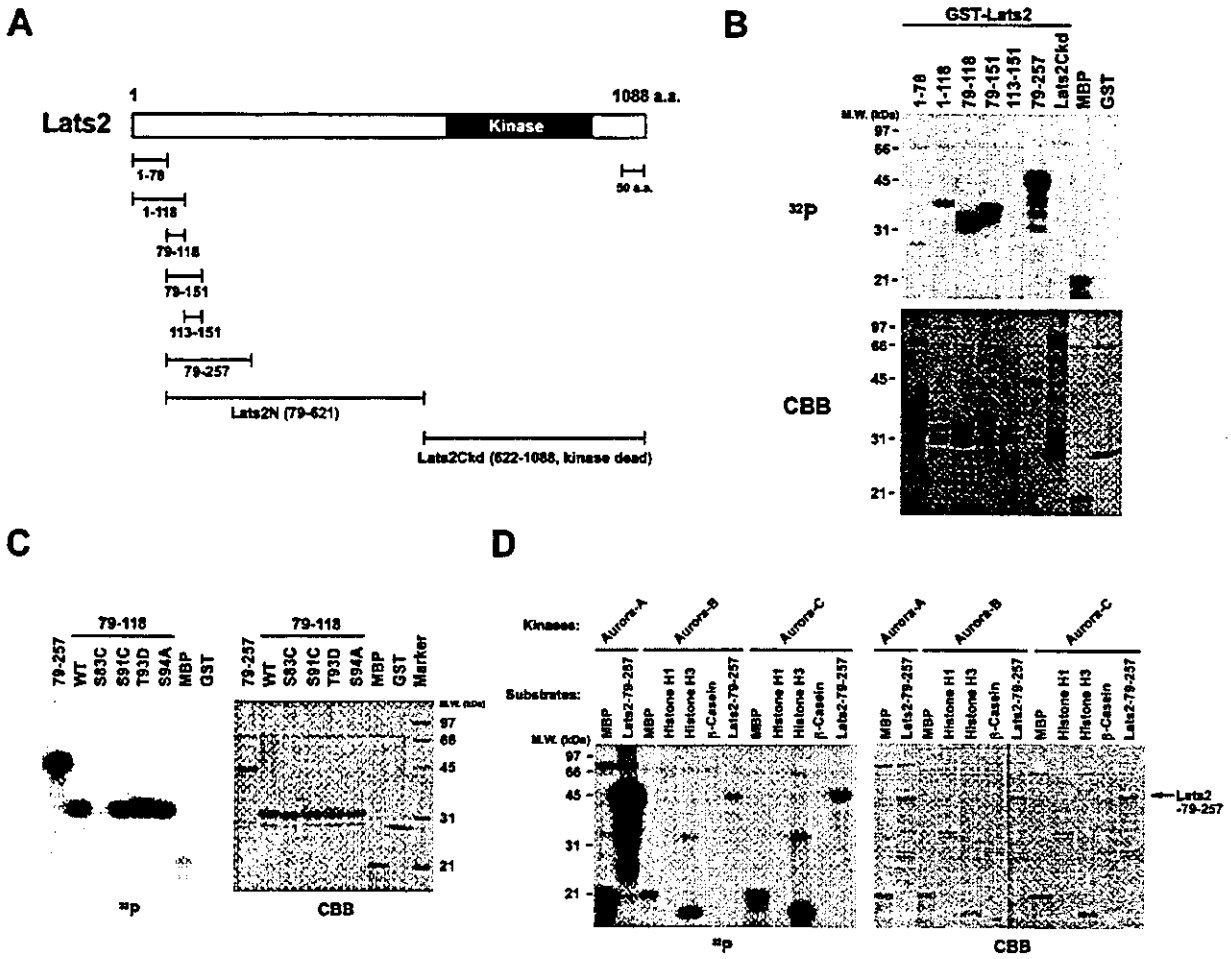

Figure 2 Recombinant Aurora-A kinase phosphorylates the S83 residue of Lats2 *in vitro*. (A) Schematic diagram of Lats2 that shows the location of the kinase domain. Beneath are the GST-fusion proteins used in the kinase reactions, namely, those containing Lats2 amino acids 1–79, 1–118, 79–118, 79–151, 113–151, 79–257, 79–621 (Lats2N) and 622–1088 (Lats2Ckd, kinase dead). (B) *In vitro* kinase reactions were performed with GST-Aurora-A and truncated GST-Lats2 proteins. The truncated GST-fusion proteins used were those containing amino acids 1–78, 1–118, 79–118, 79–151, 113–151, 79–257 and 622–1088 (Lats2Ckd) of Lats2. CBB staining shows a loading control (bottom panel). (C) An *in vitro* kinase reaction was performed with GST-Aurora-A and GST-Lats2-79-118 proteins that harbour the indicated substitutions (left panel). CBB staining shows that equal amounts of proteins were present (right panel). (D) *In vitro* kinase reactions were performed using GST-Lats2-79-257 as a substrate with the kinases GST-Aurora-A, GST-Aurora-B and GST-Aurora-C. CBB staining shows a loading control (right panel).

left panel). In addition, we found that the S83 residue is conserved not only in human Lats2 but also in mouse Lats2, mouse Lats1 and human Lats1 (data not shown). We also asked whether Aurora-B and -C can phosphorylate Lats2 as well as Aurora-A. An *in vitro* kinase assay was performed with these purified Aurora kinases using purified Lats2-79-257 as a substrate. Lats2 was phosphorylated by Aurora-B and -C but much more inefficiently than Aurora-A (Fig. 2D). These results indicate that Lats2, at least the 79–257 region, is phosphorylated predominantly by Aurora-A and weakly by Aurora-B and Aurora-C *in vitro*.

Aurora-A kinase phosphorylates the serine 83 of Lats2 *in vivo*

To confirm that S83 of Lats2 is phosphorylated by Aurora-A, we raised a specific monoclonal mouse anti-phospho-S83 antibody (3B11) by immunizing mice with a Lats2 peptide whose S83 residue is phosphorylated. The *in vitro* kinase assay was performed with wild-type Aurora-A or the kinase-dead form of Aurora-A with GST-Lats2-79-118 (WT) or GST-Lats2-79-118 (S83C) in the absence of [γ-^{32}P]ATP and analysed by Western blotting with the 3B11 antibody (Fig. 3A). When wild-type

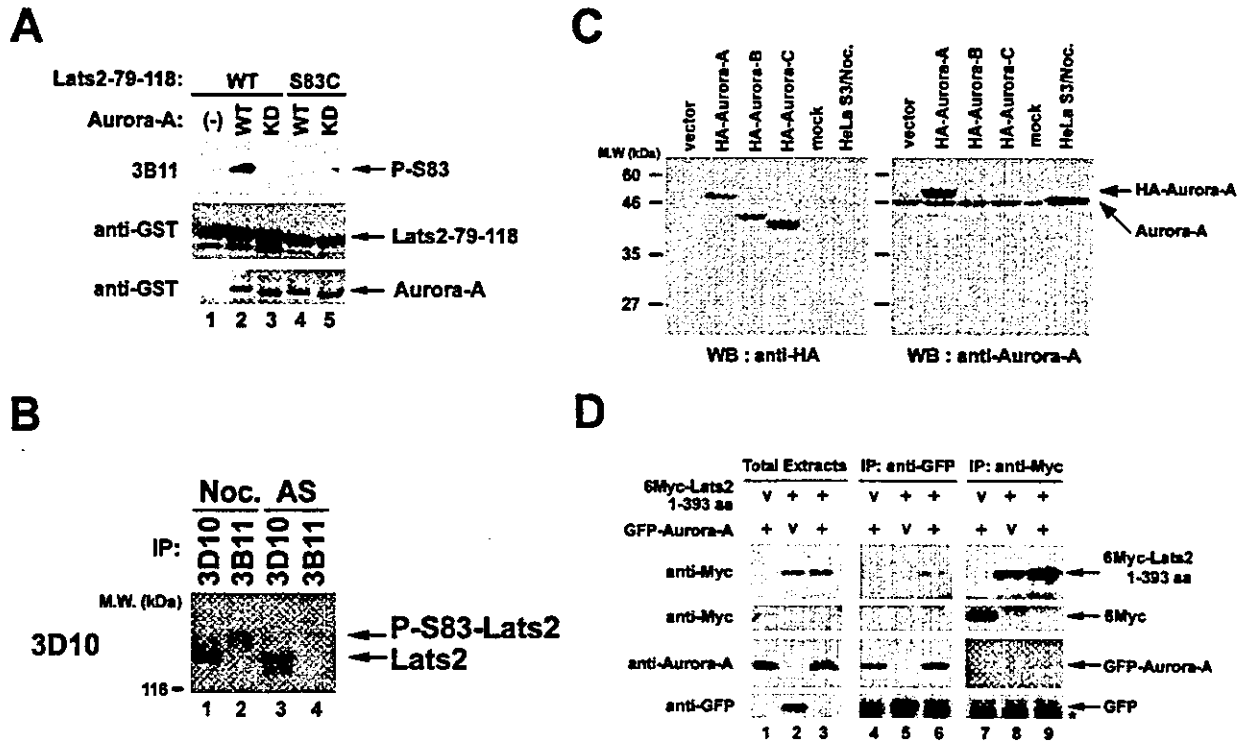

Figure 3 Lats2 is phosphorylated on S83 and interacts with Aurora-A *in vivo*. (A) Specificity of the anti-phospho-S83 monoclonal antibody (3B11). *In vitro* kinase reactions were performed with GST-Lats2-79-118-WT (lanes 1–3) or -S83C (lanes 4 and 5) using GST-Aurora-A (WT; lanes 2 and 4) or GST-Aurora-A-kinase-dead (KD; lanes 3 and 5) in the absence of [γ-^{32}P]ATP. The assays were analysed by Western blotting with the 3B11 antibody (top panel). That equal amounts of GST-Lats2-79-118 or GST-Aurora-A proteins were present was confirmed by Western blotting with anti-GST antibody (middle and bottom panels). (B) Phosphorylation state of endogenous Lats2 protein at the M phase. Endogenous Lats2 was immunoprecipitated from nocodazole-arrested M phase (Noc.) or asynchronous (AS) cell extracts with the anti-Lats2 monoclonal antibody (3D10; lanes 1 and 3) or the anti-phospho-Ser83 monoclonal antibody (3B11; lanes 2 and 4), followed by Western blotting with the 3D10 antibody. (C) Specificity of the anti-Aurora-A polyclonal antibody. 293T cells were transfected with HA-tagged Aurora-A, Aurora-B, Aurora-C or vector alone. The whole cell lysates were resolved by SDS-PAGE, followed by Western blotting with anti-HA (left panel) or anti-Aurora-A antibodies (right panel). (D) *In vivo* interaction of Lats2-1-393 with Aurora-A. 293T cells were co-transfected with 6Myc-Lats2-1-393 (lanes 2, 3, 5, 6, 8 and 9) and/or GFP-Aurora-A (lanes 1, 3, 4, 6, 7 and 9). As controls, the lysate of 293T cells transfected with empty vectors were used (V; lanes 1, 2, 4, 5, 7 and 8). GFP-Aurora-A or 6Myc-Lats2-1-393 was immunoprecipitated with the anti-GFP antibody (lanes 4–6) or anti-Myc antibody (lanes 7–9), respectively. Whole cell lysates (lanes 1–3, about 7 μg each) and immunoprecitates were resolved by SDS-PAGE, followed by Western blotting with the anti-Myc (top and 2nd panels from top) or anti-Aurora-A (3rd panel from top) or anti-GFP antibodies (bottom panel). An asterisk indicates IgG light chain.

Aurora-A was used, the 3B11 antibody specifically detected the phosphorylated form of WT Lats2-79-118 (lane 2). However, no phosphorylation of the S83 site was detected when kinase-dead Aurora-A was used (lane 3). Therefore, the 3B11 antibody is specific for the phosphorylated form of S83.

The 3B11 antibody was used to show that the S83 residue in endogenous Lats2 is phosphorylated *in vivo* in a cell cycle-dependent manner. The 3D10 antibody that recognizes Lats2 was also used. Therefore, the Lats2 proteins in lysates from nocodazole-treated or asynchronous HeLa cells were immunoprecipitated with either the 3D10 or the 3B11 antibody, followed by Western blotting using the 3D10 antibody (Fig. 3B). The 3B11 antibody immunoprecipitated the phosphorylated-S83-Lats2 protein from the nocodazole-treated cell lysate (lane 2) but not from the asynchronous cell lysate (lane 4). In contrast, the 3D10 antibody brought down equivalent amounts of Lats2 protein from each cell lysate (lanes 1 and 3), although the 3D10 antibody could not recognize the M phase-specific phosphorylated form of Lats2 in the immunoprecipitate of the 3D10 antibody (lane 1). The 3D10 antibody may be able to recognize the M phase-specific phosphorylated form of Lats2 in Western